

Annual Review of Earth and Planetary Sciences

Frontiers of Carbonate Clumped Isotope Thermometry

Katharine W. Huntington¹ and Sierra V. Petersen²

¹Department of Earth and Space Sciences, University of Washington, Seattle, Washington, USA: email: kate1@uw.edu

²Department of Earth and Environmental Sciences, University of Michigan, Ann Arbor, Michigan, USA

Annu, Rev. Earth Planet, Sci. 2023, 51:611-41

First published as a Review in Advance on March 1, 2023

The Annual Review of Earth and Planetary Sciences is online at earth.annualreviews.org

https://doi.org/10.1146/annurev-earth-031621-085949

Copyright © 2023 by the author(s). This work is licensed under a Creative Commons Attribution 4.0 International License, which permits unrestricted use, distribution, and reproduction in any medium, provided the original author and source are credited. See credit lines of images or other third-party material in this article for license information.

ANNUAL CONNECT

www.annualreviews.ora

- · Download figures
- Navigate cited references
- · Keyword search
- · Explore related articles
- · Share via email or social media



Keywords

stable isotopes, isotopologue, clumped isotopes, carbonate thermometry, geochemistry

Abstract

Carbonate minerals contain stable isotopes of carbon and oxygen with different masses whose abundances and bond arrangement are governed by thermodynamics. The clumped isotopic value Δ_i is a measure of the temperature-dependent preference of heavy C and O isotopes to clump, or bond with or near each other, rather than with light isotopes in the carbonate phase. Carbonate clumped isotope thermometry uses Δ_i values measured by mass spectrometry $(\Delta_{47}, \Delta_{48})$ or laser spectroscopy (Δ_{638}) to reconstruct mineral growth temperature in surface and subsurface environments independent of parent water isotopic composition. Two decades of analytical and theoretical development have produced a mature temperature proxy that can estimate carbonate formation temperatures from 0.5 to 1,100°C, with up to 1-2°C external precision (2 standard error of the mean). Alteration of primary environmental temperatures by fluid-mediated and solid-state reactions and/or Δ_i values that reflect nonequilibrium isotopic fractionations reveal diagenetic history and/or mineralization processes. Carbonate clumped isotope thermometry has contributed significantly to geological and biological sciences, and it is poised to advance understanding of Earth's climate system, crustal processes, and growth environments of carbonate minerals.

 Clumped heavy isotopes in carbonate minerals record robust temperatures and fluid compositions of ancient Earth surface and subsurface environments.

- Mature analytical methods enable carbonate clumped Δ_{47} , Δ_{48} , and Δ_{638} measurements to address diverse questions in geological and biological sciences.
- These methods are poised to advance marine and terrestrial paleoenvironment and paleoclimate, tectonics, deformation, hydrothermal, and mineralization studies.

1. INTRODUCTION

Stable isotope geochemistry is a foundational tool in Earth sciences, cosmochemistry, and paleobiology. For 70 years, conventional stable isotope analysis has examined processes that control the relative abundance of heavy to light isotopes in a variety of natural materials. A major innovation in the early 2000s was achieved with the development of clumped isotope geochemistry, which examines how often the heavy isotopes in a sample clump or bond together or near each other (Eiler 2007). As detailed in Section 2, clumping is quantified using the variable Δ_i , which measures the abundance of clumped isotopologue *i* containing multiple heavy isotopes, relative to the abundance predicted for a stochastic or random distribution of heavy isotopes (Wang et al. 2004). Clumped isotope theory and Δ_i measurements have been established for materials including carbon dioxide (Eiler & Schauble 2004, Affek & Eiler 2006), oxygen gas (Yeung et al. 2012), methane (Stolper et al. 2014, Wang et al. 2015, Young et al. 2017), and carbonates (Ghosh et al. 2006a, Schauble et al. 2006), and represent a new way to explore the isotopic diversity of natural materials and processes (Eiler 2013).

The most developed application of clumped isotope geochemistry is carbonate clumped isotope (Δ_{47}) geothermometry, which is based on heavy $^{13}C^{-18}O$ clumping in carbonate ions (Ghosh et al. 2006a). Δ_{47} depends on growth temperature but not on the isotopic composition of the fluid from which the carbonate mineral grew ($\delta^{18}O$ of fluid/water, or $\delta^{18}O_w$). Consequently, Δ_{47} thermometry offers a significant advantage over conventional oxygen isotope ($\delta^{18}O$) carbonate-water thermometry (e.g., Epstein et al. 1951), which depends on both temperature and $\delta^{18}O_w$. Together, measured Δ_{47} and $\delta^{18}O$ of carbonate ($\delta^{18}O_C$) can constrain both temperature and $\delta^{18}O_w$ in the many Earth surface and subsurface environments in which carbonates occur. The sensitivity of clumped isotope values to diagenesis, biological, kinetic, and other effects has also opened up exciting opportunities to quantify thermal and chemical processes in the crust, isotopic disequilibrium, and mineralization processes in biogenic and abiogenic settings.

Since the first carbonate Δ_{47} measurements nearly 20 years ago, practitioners have faced a variety of technical challenges (Huntington et al. 2009, Spencer & Kim 2015). Clumped isotope methods build on conventional C and O isotope analyses, which digest carbonate in acid to produce CO₂ for analysis via mass spectrometry or laser spectroscopy. However, carbonate clumped isotope thermometry requires order-of-magnitude better precision than conventional C and O isotope studies, on an analyte that is orders-of-magnitude lower abundance and much more sensitive to alteration. How can such high precision be achieved while limiting biases in the clumped isotopic composition introduced by sample preparation and analytical artifacts? How can Δ_{47} values be anchored to theory and standardized from one lab to another? Is there a universal relationship between Δ_{47} and formation temperature for carbonates of different origins and mineralogies? What factors, beyond temperature, affect carbonate clumping? Once determined how should apparent Δ_{47} -derived temperatures be interpreted? Solutions to some problems (long analysis time to achieve high-precision, custom-built sample purification lines) created new challenges (large sample size requirements, laborious preparation procedures, low sample throughput). Differences between performance of apparently identical mass spectrometers required lab-specific solutions, potentially exacerbating interlaboratory comparability issues.

The field of carbonate clumped isotope thermometry has matured rapidly to address these challenges. Thanks to collaborative community efforts and interlaboratory standardization, Δ_{47} -temperature calibration issues have been resolved. A solid theoretical framework has been developed for understanding equilibrium, kinetic, and other effects on carbonate clumping and the interpretation of clumped isotope values. Advances in mass spectrometer technology and automation and standardization of sample preparation procedures have led to higher-precision measurements on smaller samples and higher mass isotopologues. Lessons learned from Δ_{47} are enabling accelerated development of Δ_{48} thermometry based on $^{18}O^{-18}O$ clumping and laser-based measurements of $^{13}C^{-18}O$ clumping (Δ_{638}). Δ_{47} thermometry has progressed past early growing pains into the productive application phase of proxy development, with Δ_{48} and Δ_{638} close behind. No longer a new method, carbonate clumped isotope paleothermometry should be considered a rigorously calibrated, thermodynamically based temperature proxy with a multitude of scientific applications spanning the fields of tectonics, paleoclimate, paleobiology, metamorphic geology, planetary science, and more.

As technical issues are resolved and applications expand, it is a good time to take stock of the state of the field and envision places where carbonate clumped isotope paleothermometry can be uniquely useful going forward. Additionally, as the number of laboratories purchasing off-the-shelf instruments that can perform automated carbonate clumped isotope sample preparation and measurements is increasing, more and more new users are trying to catch up on two decades worth of literature. Here, we build on previous reviews describing clumped isotope theory (Eiler 2007, 2013), application to paleoclimate (Eiler 2011, Affek 2012) and tectonics (Huntington & Lechler 2015), and technological advancements (Spencer & Kim 2015). The following sections describe principles of clumped isotope geochemistry and measurement techniques employed and in development, as well as key past contributions and future opportunities for carbonate clumped isotope thermometry to address scientific challenges across multiple disciplines of geological and biological sciences. To help this review be a teaching resource and reference for students, experts, and anyone in between, the **Supplemental Companion** provides historical context, supporting calculations, and literature sources underlying key developments mentioned in the main text.

Supplemental Material >

2. BACKGROUND

2.1. Isotopologues, Clumping, and Temperature Dependence of Δ_i Values

Isotopologues are molecules of the same compound that have the same chemical formula but vary in their isotopic composition. For example, stable isotopes of carbon (12 C, 13 C) and oxygen (16 O, 17 O, 18 O) combine to form isotopologues of carbon dioxide such as 12 C 16 O₂ (the isotopically lightest and most abundant isotopologue) and 12 C 18 O 16 O (an example of a singly substituted isotopologue having one heavy isotope, 18 O, substituted for a light isotope, 16 O) (**Figure 1***a,b*). Ratios (*R*) of heavy to light stable isotopes in a sample define the sample's bulk isotopic composition, which is described relative to the isotopic ratio of a standard using delta notation, e.g.,

$$\delta^{18}O = \frac{\binom{^{18}O_{\text{samp}}}{^{16}O_{\text{samp}}}}{\binom{^{18}O_{\text{std}}}{^{16}O_{\text{std}}}} - 1 = \frac{R_{\text{samp}}^{18}}{R_{\text{std}}^{18}} - 1$$
 1.

and

$$\delta^{13}C = \frac{\binom{{}^{13}C \text{ samp}}{{}^{12}C \text{ samp}}}{\binom{{}^{13}C \text{ std}}{{}^{12}C \text{ srd}}} - 1 = \frac{R_{\text{samp}}^{13}}{R_{\text{std}}^{13}} - 1.$$
 2.

Typically, delta values are multiplied by 1000 to report in permil (%).

Due to differences in isotopic masses and/or thermodynamic properties, heavy or light isotopes are preferentially incorporated (fractionated) into one phase (e.g., solid, liquid, or across a chemical reaction) relative to another. The magnitude of this fractionation is a function of temperature and other variables. Precise measurement of the bulk stable isotopic compositions of natural materials to quantify isotopic fractionations and the myriad processes they record grew rapidly in the 1950s to become the mainstay of stable isotope geochemistry. Of particular relevance, oxygen

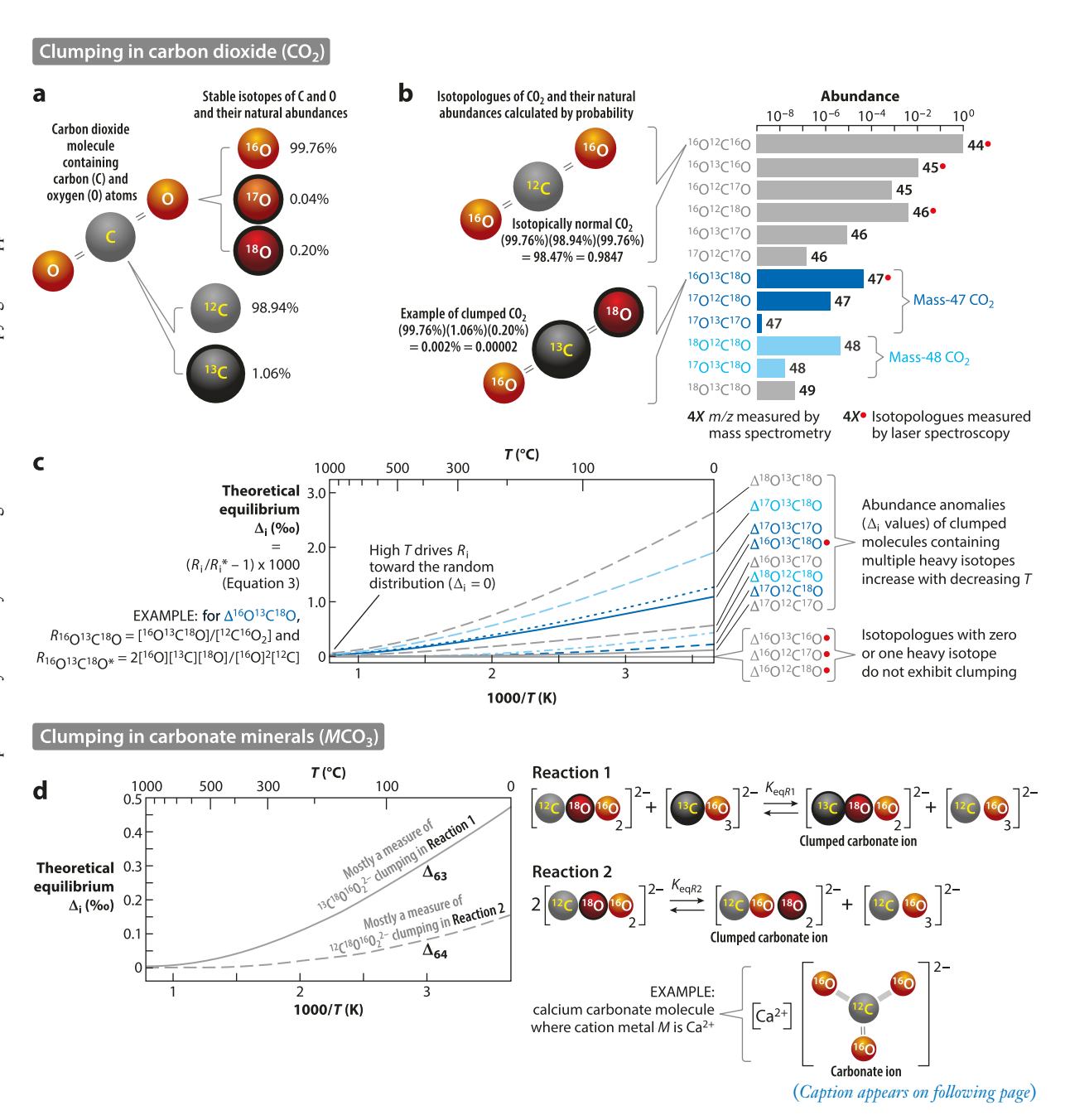


Figure 1 (Figure appears on preceding page)

Basic principles surrounding abundances and temperature dependence of isotopes and isotopologues illustrated for CO₂ and MCO₃. (a) Stable isotopes of carbon (12 C, 13 C) and oxygen (16 O, 17 O, 18 O) combine to form CO₂. (b) Natural abundances of the 12 isotopologues of CO₂ are calculated based on the abundance of individual isotopes using probability rules. Rare clumped isotopologues contain multiple heavy isotopes. Mass spectrometry measurements combine all isotopologues of the same mass to charge ratio (m/z), whereas laser spectroscopy measures individual isotopologue abundances. Note log scale on the abundance axis. (c) Abundance anomalies (Δ_i values) relate the ratio of isotopologue i relative to the unsubstituted isotopologue (R_i) to the same ratio calculated for a random distribution of isotopes among isotopologues (R_i *). Theoretical equilibrium Δ_i values of clumped molecules increase with decreasing temperature (T). Panel c theoretical equilibrium Δ_i calculations for CO₂ isotopologues are from Wang et al. (2004), updated by Petersen et al. (2019). Panel d theoretical equilibrium clumping values for calcite (Δ_{63} and Δ_{64}) are from Hill et al. (2014). Δ_{63} is mostly a measure of clumping in Reaction 1 [12 C 18 O 16 O 2 - 2 + 13 C 16 O 3 - 2 2 + 13 C 16 O 3 - 2 + 12 C 16 O 3 - 2 - 13 , and Δ_{64} is mostly a measure of clumping in Reaction 2 [212 C 18 O 16 O 2 - 2 + 12 C 16 O 3 - 2 - 2 + 12 C 16 O 3 - 3]. 4X and 4X-dot in the symbol key refer to m/z, where X = 4, 5, 6, 7, 8, or 9). Abbreviations: K_{eq} , equilibrium constant; K_{eq} /K*, normalized equilibrium constant; M, metal; T, temperature.

isotope thermometry leveraged the dependence of $\delta^{18}O_C$ in carbonate materials on their formation temperature (T) and secondarily on $\delta^{18}O_w$ of the fluid from which the mineral grew. (For an excellent guide to the field of light stable isotope geochemistry, see Sharp 2017.)

For many decades, stable isotope geochemistry was not much concerned with clumped isotopologues, which have more than one heavy isotope substituted for light isotopes (e.g., $^{13}C^{18}O^{16}O$) (Eiler 2007). Early workers recognized that multiply substituted isotopologues have distinct thermodynamic properties and should exhibit different fractionations than singly substituted isotopologues, but they lacked a way to effectively measure abundances of these extremely rare molecules in natural materials. That changed when the first measurements of clumping in atmospheric CO_2 were made at Caltech in the early 2000s (Eiler & Schauble 2004, Affek & Eiler 2006). Foundational publications on clumped isotope theory (Wang et al. 2004, Schauble et al. 2006, Guo et al. 2009) and observations, especially for carbonates (Ghosh et al. 2006a), launched the study of clumped isotopes as a new frontier of geochemistry.

Analogous to δ notation, isotopic clumping is characterized using the variable Δ_i , which describes the enrichment of a given multiply substituted isotopologue i relative to the random (stochastic) distribution (Wang et al. 2004):

$$\mathbf{\Delta}_{i} = \left(\frac{R_{i}}{R_{i}^{*}} - 1\right) \times 1000, \tag{3}$$

where R_i quantifies the abundance of the multiply substituted isotopologue of interest, i, divided by the abundance of the isotopologue having no heavy isotopes (e.g., $R_{13C18O16O} = [^{13}C^{18}O^{16}O]/[^{12}C^{16}O_2]$). Unlike in δ notation, R_i is not compared to the same ratio in a standard material like Vienna Peedee Belemnite (VPDB). Instead, it is compared to R_i^* , the same ratio (isotopologue i relative to the unsubstituted isotopologue), calculated for a pool of molecules with the same bulk isotopic composition (i.e., same abundance of each individual isotope in the total pool, e.g., $[^{18}O]$) but a random distribution of isotopes among isotopologues. When the distribution of heavy isotopes among isotopologues is dictated by random chance (also known as stochastic or disordered distribution), the expected abundance of any clumped isotopologue can be calculated based on the abundance of individual isotopes using basic probability theory (**Figure 1**b; **Supplemental Companion 1**). Using an analogy with a pair of dice, this is like calculating the probability of rolling two fives, given that a five occurs on one of six sides. Importantly, Δ_i values are independent of bulk isotopic composition (**Supplemental Companion 2**).

Based on Equation 3, a material with a stochastic distribution of isotopes has a Δ_i value equal to 0 because R_i equals R_i^* . Because clumped molecules have lower vibrational energies and are therefore more thermodynamically stable than molecules that contain zero or one heavy isotope

(see the rule of the mean discussions in Eiler 2007 and Huntington & Lechler 2015), there is a thermodynamic preference for more clumped molecules to occur than would be predicted by random chance, leading to Δ_i values greater than zero in most natural materials.

Molecular theory predicts that at equilibrium, the prevalence of clumped molecules containing two or more heavy isotopes should decrease as T increases, due to the effects of increased entropy at higher temperatures overcoming the bond ordering preference (Eiler 2007). Calculations illustrate the equilibrium temperature dependence of isotopic clumping in gaseous molecules including CO_2 and CH_4 (e.g., Wang et al. 2004, Ma et al. 2008, Piasecki et al. 2016) (**Figure 1**c). Similar calculations (e.g., Schauble et al. 2006, Hill et al. 2014) for equilibrium clumping behavior in carbonate minerals (MCO_3 , where M is a metal such as Ca^{2+}), which are more readily preserved in the geologic record, form the theoretical basis of carbonate clumped isotope geothermometry.

2.2. Carbonate Clumped Isotope Geothermometry

From the first clumped isotope measurements in atmospheric CO_2 samples (Eiler & Schauble 2004), clumped isotope geochemistry applications quickly turned to carbonate geothermometry (Ghosh et al. 2006a) for practical and scientific reasons. Carbonate minerals are formed in a multitude of environments (marine, terrestrial, subsurface, diagenetic) through biogenic and abiogenic processes and can be preserved over millions of years with their chemistry unchanged, giving them the potential to record ancient environmental signals. Methods for digesting carbonates in acid to produce CO_2 for $\delta^{13}C$ and $\delta^{18}O$ analysis were well established and readily portable to clumped isotope studies.

Unlike δ^{18} O thermometry, which deals with heterogeneous equilibrium involving the amounts of heavy isotopes in two phases (carbonate and water), carbonate clumped isotope thermometry considers homogeneous equilibrium exchange of heavy isotopes within a single phase (carbonate) via ion exchange reactions such as the following:

$${}^{12}C^{18}O^{16}O_2{}^{2-} + {}^{13}C^{16}O_3{}^{2-} \rightleftarrows {}^{13}C^{18}O^{16}O_2{}^{2-} + {}^{12}C^{16}O_3{}^{2-}$$
 Reaction 1.

and

$$2^{12}C^{18}O^{16}O_2^{2-} \rightleftharpoons {}^{12}C^{16}O^{18}O_2^{2-} + {}^{12}C^{16}O_3^{2-}$$
. Reaction 2.

Whether in CO_3^{2-} , as above, or in analogous exchange reactions between molecules of CO_2 , heavy isotopes prefer to clump together to form multiply substituted ions (right side) relative to the randomly distributed configuration of isotopes among singly substituted ions (left side). At thermodynamic equilibrium, decreasing temperature drives these reactions to the right, increasing the abundance of clumped ions relative to singly substituted ions (**Figure 1***c*,*d*).

Stated another way, the equilibrium constants, K_{eq} (defined as follows), of these reactions are proportional to temperature:

$$K_{\text{eqR1}} = \frac{\left[^{13}\text{C}^{18}\text{O}^{16}\text{O}_{2}^{2^{-}}\right]\left[^{12}\text{C}^{16}\text{O}_{3}^{2^{-}}\right]}{\left[^{12}\text{C}^{18}\text{O}^{16}\text{O}_{2}^{2^{-}}\right]\left[^{13}\text{C}^{16}\text{O}_{3}^{2^{-}}\right]}$$
4.

and

$$K_{\text{eqR2}} = \frac{\left[^{12}\text{C}^{16}\text{O}^{18}\text{O}_{2}^{2-}\right]\left[^{12}\text{C}^{16}\text{O}_{3}^{2-}\right]}{\left[^{12}\text{C}^{18}\text{O}^{16}\text{O}_{2}^{2-}\right]^{2}}.$$
5.

Similarly to $K_{\rm eq}$, the $\Delta_{\rm i}$ value of a clumped isotopologue of CO₂ or CO₃²⁻ (e.g., $\Delta_{\rm 13C18O16O16O}$) relates the occurrence of doubly substituted isotopologues to singly substituted isotopologues. Thus, $\Delta_{\rm i}$ provides an estimate of the equilibrium constant $K_{\rm eq}$ and therefore also an estimate of temperature (Wang et al. 2004) (**Figure 1***c,d*; **Supplemental Companion 3**).

2.3. Δ_i-Based Temperatures and Fluid Compositions

One of the most powerful aspects of carbonate clumped isotope geochemistry is its ability to determine mineral formation temperature independent of $\delta^{18}O_w$ of the growth fluid. In conventional (singly substituted) $\delta^{18}O$ thermometry, measured $\delta^{18}O_C$ values depend on both the growth T and growth fluid $\delta^{18}O_w$. $\delta^{18}O_w$, which is rarely preserved in the geologic record, must be known/assumed to accurately calculate formation temperature. Qualitatively, when there are more heavy isotopes in the growth fluid or when temperatures are colder, more heavy isotopes are incorporated into the carbonate. Quantitatively, the equilibrium relationship among T, $\delta^{18}O_C$, and $\delta^{18}O_w$ has been determined for synthetically precipitated carbonates of different mineralogies (e.g., Kim & O'Neil 1997, Kim et al. 2007) and for different types of biogenic carbonates (e.g., Grossman & Ku 1986, Bemis et al. 1998).

In the clumped isotope (multiply substituted) system, temperature is inferred from a single, measurable parameter (Δ_i), eliminating uncertainty due to assumptions about poorly quantified $\delta^{18}O_w$. Further, the Δ_i -based temperature can be paired with $\delta^{18}O_C$, which is measured simultaneously, to directly calculate $\delta^{18}O_w$ (Eiler 2011).

3. CARBONATE CLUMPED ISOTOPE THERMOMETRY TECHNIQUES

3.1. Converting MCO₃ to Pure CO₂

Clumped isotope analytical techniques build on methods first established in the 1950s for conventional δ^{18} O thermometry (McCrea 1950, Swart et al. 1991). First, MCO $_3$ is converted to CO $_2$ by digestion in phosphoric acid (Ghosh et al. 2006a) (**Figure 2a**). Highly concentrated H $_3$ PO $_4$ ($\geq 105\%$) is used to minimize the number of water molecules sample CO $_2$ can interact with, as CO $_2$ and water readily exchange isotopes, erasing the original clumped isotope signature. Acid temperature is held constant to control isotopic fractionation that occurs when one oxygen atom is lost in the conversion of MCO $_3$ to CO $_2$. This acid digestion fractionation produces CO $_2$ with δ^{18} O and clumped isotope values that are isotopically lighter than, but proportional to, those in the reactant carbonate (e.g., Kim et al. 2007, Guo et al. 2009, Defliese et al. 2015a, Müller et al. 2017). In both δ^{18} O and Δ_{47} , the magnitude of this fractionation increases as acid temperature increases, hence the need to maintain constant, known acid temperature during reaction (**Supplemental Companion 4**).

Multiple steps are taken to limit interaction between produced CO_2 and ambient water, which can erase the original clumped signal. One or more cool traps $(-80^{\circ}C)$ are used to separate water produced during carbonate digestion $(MCO_3 + H_3PO_4 \rightarrow CO_2 + H_2O + M_3(PO4)_2)$ and ambient water vapor not removed by vacuum pumps (cryogenic separation) from sample CO_2 , which is frozen at liquid nitrogen temperatures $(-180^{\circ}C)$ for the duration of the reaction. Further purification to remove isobaric interferences (Section 3.2) is achieved by passing sample CO_2 through Porapak Q material in a static trap or gas chromatography column (**Figure 2***b*). Finally, pure CO_2 is analyzed by an isotope-ratio mass spectrometer (IRMS) or isotope-ratio laser spectrometer (IRLS) (**Figure 2***c*).

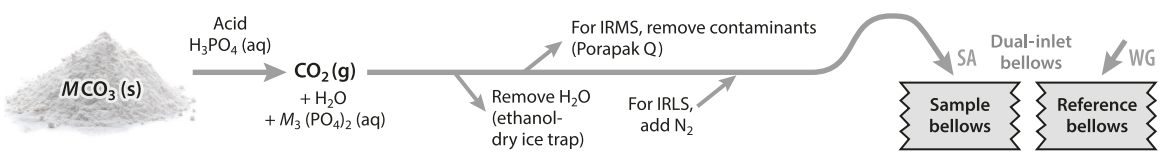
3.2. Clumped Isotope Analysis by Isotope-Ratio Mass Spectrometry

Most carbonate clumped isotope studies to date have analyzed MCO_3 -derived CO_2 via IRMS (e.g., Ghosh et al. 2006a, Eiler 2007, Huntington et al. 2009). A magnetic sector IRMS accelerates a stream of ionized sample CO_2 molecules (CO_2^+) over an electric potential, magnetically separates the stream into ion beams of different mass-to-charge ratios (m/z), and measures their currents on an array of ion collectors (**Figure 2**c, left). Molecules of lower mass bend more in

the magnetic field and are on the inside curve of the array (Figure 2c). The IRMS integrates signals of all isotopologues of the same cardinal m/z into a single beam. Therefore, the Δ_i value of a single clumped isotopologue (e.g., $\Delta_{13C18O16O}$ quantifying $^{16}O^{13}C^{18}O$) cannot be determined independently of contributions from other CO₂ isotopologues of the same mass (e.g., ¹⁷O¹²C¹⁸O and ¹⁷O¹³C¹⁷O). All mass-47 CO₂ isotopologues are multiply substituted and thus temperature dependent. Δ_{47} is therefore proportional to temperature. Because $^{16}\mathrm{O}^{13}\mathrm{C}^{18}\mathrm{O}$ makes up $\sim 97\%$ of m/z-47 CO₂, Δ_{47} is approximately equal to $\Delta_{13C18O16O}$.

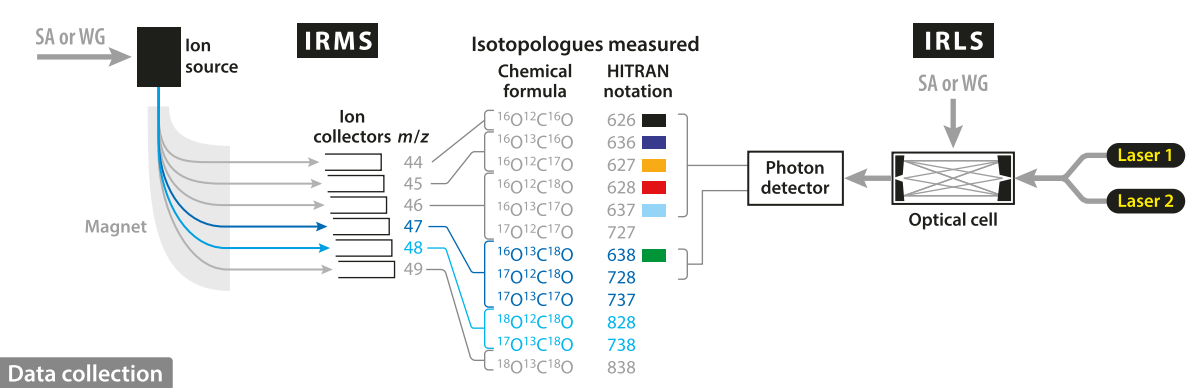
Sample preparation

Purify CO₂ and prepare gas analytes (SA and WG) for transfer to analyzer React carbonate in acid to produce CO₂

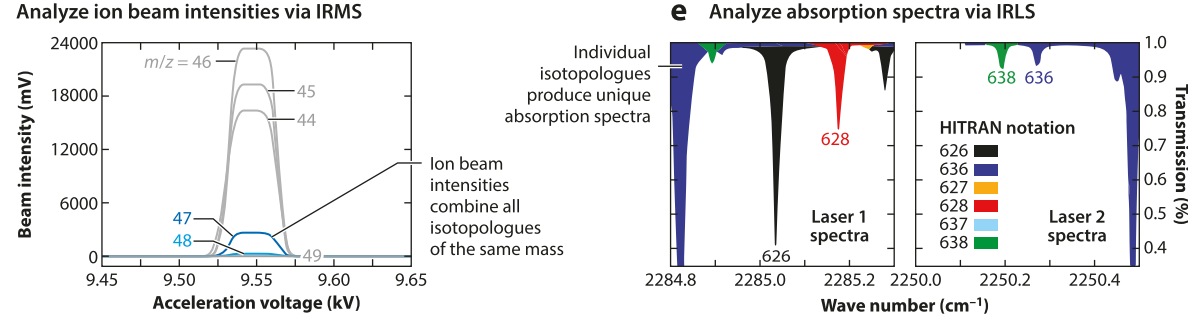


Analyzer

Analyze isotopologue ratios via isotope-ratio mass spectrometer (IRMS) or laser spectrometer (IRLS)



Analyze ion beam intensities via IRMS



Calculated Δ_i

Calculate clumped CO₂ values from IRMS

$$\Delta_{47} = (R_{47}/R_{47}^* - 1) \times 1000$$

$$\Delta_{48} = (R_{48}/R_{48}^* - 1) \times 1000$$

Calculate clumped CO₂ values from IRLS

$$\Delta_{638} = -1000 \text{ In } \frac{[638] [626]}{[636] [628]}$$
(Caption appears on following page)

Basics of carbonate clumped isotope sample preparation and analysis using an IRMS or IRLS. (a) Carbonate sample is reacted in phosphoric acid to produce CO_2 . (b) Sample CO_2 is purified, and prepared sample (SA) and calibrated working gas (WG) analytes are introduced into respective bellows of a dual-inlet system. (c, left) An IRMS analyzes isotopologue ratios by accelerating a stream of ionized CO_2 molecules over an electric potential, magnetically separating the stream into ion beams of different mass-to-charge ratios (m/z), and measuring their currents on an array of ion collectors. (c, right) An IRLS passes laser-emitted infrared radiation through an optical cell containing CO_2 (diluted with N_2) to produce absorption spectra of specific isotopologues, and the intensity of the transmitted radiation is measured using a photon detector. (d) IRMS data collection combines signals of all isotopologues of the same m/z into a single beam, and beam intensities at peak center are compared. (e) IRLS measures individual isotopologue abundances, and peak areas are compared. (f) Clumped isotope abundance anomalies (Δ_i) are calculated from IRMS beam ratios (R_{47} and R_{48}) and their associated stochastic ratios (R_{47} and R_{48}). (See **Supplemental Companion 13** for details of IRMS-based calculations.) (g) Clumped isotope abundance anomalies (Δ_i) are calculated from IRLS peak ratios of individual isotopologues (Wang et al. 2020). HITRAN notation (e.g., 638) combines the second digits of each atom's mass to define an isotopologue. Abbreviations: HITRAN, High-Resolution Transmission; IRLS, isotope-ratio laser spectrometer; IRMS, isotope-ratio mass spectrometer; M, metal; R, ratio.

 Δ_{47} is defined as

$$\Delta_{47} = \begin{pmatrix} \frac{i_{47}}{i_{44}} \\ \frac{i_{47*}}{i_{44*}} - 1 \end{pmatrix} \times 1000 = \left(\frac{R_{47}}{R_{47*}} - 1 \right) \times 1000.$$
 6.

Following Equation 3, R_{47} relates the occurrence of mass-47 isotopologues to the base $^{12}C^{16}O_2$ (m/z 44) molecule measured via beam intensities (e.g., $R_{47} = [m/z \ 47]/[m/z \ 44]$ or as currents, $= i_{47}/i_{44}$). R_{47*} is the ratio $[m/z \ 47]/[m/z \ 44]$ that would be expected for the random or stochastic distribution of isotopes among isotopologues, which is calculated based on the R_i values of individual isotopes using probability theory (**Supplemental Companion 1**). R_i values are also used to determine the bulk isotopic composition ($\delta^{13}C$, $\delta^{18}O$) as well as other clumped species (Δ_{48} and Δ_{49}). Other definitions of Δ_{47} prevalent in the literature include a correction for mass 45 and 46. The 45 and 46 terms are not needed (Daëron et al. 2016, Saenger et al. 2021) provided a uniform set of parameters (Schauer et al. 2016, Petersen et al. 2019) is used to calculate both bulk and clumped isotopic compositions (**Supplemental Companion 5**).

Achieving precisions more than 10 times better than conventional C and O isotope studies on extremely small m/z 47-49 beam signals requires traditional IRMS techniques to be modified (Spencer & Kim 2015, and references therein). More stringent sample purification is needed to avoid interference from isobaric contaminants (e.g., S compounds, organics with m/z 47–49) on these small beams, and higher-ohm resistors are used to increase beam signals on the m/z 47-49 ion collectors. The effects of secondary ions and related bulk composition-dependent nonlinearity between measured and real R₄₇ values must be corrected empirically [for example, with correction schemes involving equilibrated CO2 and/or pressure baseline background measurements (e.g., He et al. 2012)] or removed using engineering solutions (e.g., Dennis et al. 2019) (Supplemental Companion 6). As with conventional δ^{13} C and δ^{18} O analysis, a dual-inlet system for sample introduction aids in high-precision analysis by ensuring analytical stability with frequent sample-working gas (WG) reference comparisons. However, orders-of-magnitude longer measurement (integration) time is needed to accumulate necessary statistics on the smaller beams of the clumped isotopologues (Supplemental Companion 7). This longer measurement time, whether accomplished by analyzing a single gas for a long period (Huntington et al. 2009) or combining sample-WG comparison cycles from multiple smaller aliquots of sample gas created from multiple acid reactions (Schmid & Bernasconi 2010), ends up requiring orders-of-magnitude more sample material than traditional carbon and oxygen isotope measurement to achieve useful precision. Finally, fragmentation and recombination reactions in the IRMS source cause isotopic scrambling that drives Δ_{47} composition of analyte CO₂ toward the random distribution ($\Delta_i = 0$), reducing the measured contrast between low and high Δ_{47} values (scale compression) and causing

an effective loss of resolution for a given measurement precision (**Supplemental Companion 6**). Combatting these effects requires a multi-point calibration in both bulk composition space (δ^{47}) and clumped isotope space (Δ_{47}) that takes up valuable analytical time (see Section 3.4).

3.3. Clumped Isotope Analysis by Isotope-Ratio Laser Spectroscopy

Recently, IRLS systems have been used to analyze the abundance of clumped isotopologues in CO_2 (Prokhorov et al. 2019, Wang et al. 2020), including CO_2 derived from MCO_3 (Yanay et al. 2022). An IRLS passes laser-emitted infrared radiation through an optical cell containing sample CO_2 (diluted with N_2) to produce absorption spectra of specific isotopologues (**Figure 2**c, right). Optical cell temperature and pressure are controlled, and lasers are tuned to scan a spectral region known to resonate with the molecules of interest and be free of spectral interference by likely contaminants. A detector measures the intensity of the transmitted radiation, and the signal is digitally processed using spectral fitting to calculate isotopologue abundances of the sample gas.

Frequency shifts in absorption lines depend on molecular mass and on the geometric arrangement of mass within analyte molecules, and so they are unique for each isotopologue, while absorption strength is proportional to isotopologue concentration. Because each isotopologue has a unique rotation-vibration spectrum, isotopologue abundances can be quantified independently, unlike IRMS measurements where isotopologues of the same mass are combined (**Supplemental Companion 8**).

Instead of determining Δ_{47} , laser spectroscopy directly calculates the equilibrium constant of Reaction 1 in a quantity abbreviated as Δ_{638} [where 638 refers to the second digit of each isotope in the isotopologue, following spectroscopic High-Resolution Transmission (HITRAN) database notation], defined as follows:

$$\begin{split} \Delta_{638} &= -1000 \ln \left(\frac{K_{\text{eq}R1}}{K_{\text{eq}R1^*}} \right) = -1000 \ln \left(\frac{[\text{O}^{16}\text{C}^{13}\text{O}^{18}][\text{O}^{16}\text{C}^{12}\text{O}^{16}]}{[\text{O}^{16}\text{C}^{13}\text{O}^{16}][\text{O}^{16}\text{C}^{12}\text{O}^{18}]} \right) \\ &= -1000 \ln \left(\frac{[638][626]}{[636][628]} \right). \end{split}$$
 7.

 $\delta^{13}C$ and $\delta^{18}O$ can be simultaneously quantified using isotopologues containing the relevant isotopes.

As with IRMS measurement, carbonate must first be digested in acid to produce CO_2 , interaction of sample gas with water must be avoided, and dual-inlet gas introduction is used to enable rapid and repeated sample-reference gas comparison. However, IRLS analysis does not require sample purification to remove isobaric contaminants because absorption line position does not solely depend on mass. Whereas IRMS systems are approaching their technical limits in terms of precision and sample size, IRLS-based CO_2 clumped isotope analysis is in the early stages of development with further technical improvements on the horizon, including the potential of concurrent measurement of additional singly substituted and clumped isotopologues of CO_2 [e.g., Δ_{828} analogous to Δ_{48} (Prokhorov et al. 2019); $\delta^{17}O$]. Currently, the IRLS system developed by Wang et al. (2020) and Yanay et al. (2022) produces Δ_{638} , δ^{13} , and $\delta^{18}O$ data that are competitive in quality and sample size with the best IRMS systems but collected more rapidly (**Supplemental Companion 7**).

3.4. Standardization of Bulk Isotope and Clumped Isotope Δ_i Values

Clumped isotope standardization builds on established approaches for standardizing bulk C and O isotope ratios measured in carbonate-derived CO₂. In traditional nonclumped isotope systems, calibrated values are achieved by co-analysis of international carbonate standards such as NBS18,

NBS19, and LSVEC (or secondary standards that have been calibrated against them) with defined compositions relative to the VPDB or Vienna Standard Mean Ocean Water (VSMOW) scale. A simple linear empirical transfer function (ETF) between $\delta^{18}O$ or $\delta^{13}C$ values measured relative to the mass spectrometer WG and true $\delta^{18}O$ or $\delta^{13}C$ values established relative to VPDB or VSMOW converts measured CO_2 compositions back into solid $CaCO_3$ space, regardless of reaction temperature, as long as acid temperature is held constant across samples and standards.

Because carbon in the reactant MCO_3 is completely converted to CO_2 , $\delta^{13}C$ values of the reactant XCO_3 and product CO_2 should be identical. Therefore, for $\delta^{13}C$, the ETF is very close to a 1:1 line, with deviations due to small inaccuracies in defined WG composition and instrument drift. In the case of $\delta^{18}O$, the slope is also close to 1, but the intercept is much greater (\sim 8–9‰) because the ETF additionally accounts for the acid digestion fractionation that occurs as one of three oxygen atoms is removed during acid digestion. Product CO_2 has higher $\delta^{18}O$ than reactant solid MCO_3 because bonds containing ^{16}O are less stable and more likely to be broken during acid digestion than bonds containing ^{18}O (Supplemental Companion 9).

Key steps in calibrating Δ_{47} values are similar in that they relate measured values to assigned true values for standard materials accepted by the international community and account for fractionation between MCO_3 and CO_2 during acid digestion. Unlike the anchors of the $\delta^{18}O$ and $\delta^{13}C$ systems (VSMOW and VPDB), for which the absolute abundance of heavy isotopes has been defined by the International Atomic Energy Agency, the anchors for the clumped isotope system are equilibrated CO_2 gases for which the theoretical clumped isotope value is calculated (Dennis et al. 2011). For a given equilibration temperature, the theoretical equilibrium abundance of each isotopologue is calculated assuming a gas with bulk composition of VPDB and a stochastic distribution of heavy isotopes across all isotopologues (Wang et al. 2004, Petersen et al. 2019) (Supplemental Companion 3). Isotopologues are combined to calculate theoretical equilibrium Δ_{47} or Δ_{48} values Δ_{47-TE} and Δ_{48-TE} .

 CO_2 anchors corresponding to a range of $\Delta_{i\text{-TE}}$ and bulk isotopic compositions are created and equilibrated to known temperatures and are analyzed interspersed with sample unknowns. CO_2 is heated [heated gases, usually 1000°C or as low as $\sim 200^{\circ}\text{C}$ (EL-Shenawy & Kim 2019)] or equilibrated with water [equilibrated gases, usually $25\text{--}30^{\circ}\text{C}$, but sometimes $4\text{--}60^{\circ}\text{C}$ (Kelson et al. 2017)] to create anchors with $\Delta_{i\text{-TE}}$ values near stochastic abundances for higher-temperature CO_2 and exceeding stochastic abundances for lower-temperature equilibration. The measured Δ_i values and bulk isotopic compositions of these gas standards are used to convert sample unknowns into an interlaboratory reference frame [the absolute reference frame or carbon dioxide equilibrium scale (CDES) ($\Delta_{47\text{-CDES}}$)]. This conversion corrects for (a) the bulk-composition-dependent nonlinearity in R_{47} and (b) scale compression by stretching Δ_i values into theoretical equilibrium space analogous to the way $\delta^{18}O$ and $\delta^{13}C$ are projected into VSMOW and VPDB space, using a two-step process defined by Dennis et al. (2011) or more recently using a one-step process that is mathematically equivalent (Daëron 2021) (Supplemental Companion 9). Several programs exist to make these calculations (John & Bowen 2016, Schauer et al. 2016, Petersen et al. 2019, Daëron 2021).

Similar to δ^{18} O, CO₂ produced by acid digestion of MCO₃ has a higher clumped isotopic composition than the carbonate reactant because bonds containing 18 O are stronger and less likely to be broken. The magnitude of this fractionation depends on the acid digestion temperature. Different experimental setups use different reaction temperatures (initially 25°C in individual vials, now more commonly 70 or 90°C in a common acid bath or individual vials), so this difference

¹Supplemental Table 1 presents recalculations for $\Delta_{48\text{-TE}}$ carried out identically to those described in Petersen et al. (2019) that were not included in the original publication.

must be accounted for when reporting and comparing Δ_i values between labs and instruments, just as the standard scale (VPDB, VSMOW) used must be reported with δ^{18} O or δ^{13} C values.

Clumped isotope data are increasingly normalized to carbonate reference materials for which community-accepted Δ_{47} values are defined and ultimately referenced back to the gas-based CDES reference frame (Bernasconi et al. 2018, 2021). This carbonate-based reference frame [Intercarb-carbon dioxide equilibrium scale (I-CDES)] is more similar to bulk isotope correction schemes and should be mathematically identical to and interchangeable with CDES, although small differences remain (Bernasconi et al. 2021). The I-CDES approach benefits from equal treatment of samples and standards, but it currently is based on carbonates that span a smaller range of bulk compositions and Δ_i values than achievable using equilibrated gases, which can lead to larger propagated errors. Analogous CDES and I-CDES approaches have been used to standardize other clumped isotope systems including Δ_{48} and Δ_{638} (Fiebig et al. 2019, Yanay et al. 2022).

3.5. Converting Carbonate Clumped Isotope Δ_i Values to Temperature

The final step of most carbonate clumped isotope studies is to convert Δ_i values to temperature $(T\Delta_i)$. Numerous studies have produced empirical $T-\Delta_{47}$ calibrations that relate Δ_i values measured in natural, synthetic, biogenic, and abiogenic carbonates of different mineralogies to their known growth temperatures (e.g., Petersen et al. 2019, and references therein) (Figure 3). Early apparent differences in the T- Δ_{47} relationship between labs (Ghosh et al. 2006a, Dennis & Schrag 2010) have largely been resolved (Kelson et al. 2017, Petersen et al. 2019, Anderson et al. 2021) (Supplemental Companion 10), with more consistent methods of sample preparation and cleaning, increased sample replication, better treatment of uncertainties, and improved interlaboratory agreement through adoption of uniform calculation methods and standardization to the CDES and I-CDES reference frames. $T-\Delta_{47}$ data are now converging across a range of mineralogies, bulk compositions, sample types, and sample preparation and analysis methods, suggesting a single broadly applicable carbonate clumped isotope thermometer calibration. Additional data could reveal mineralogical differences [e.g., for dolomite (Anderson et al. 2021)] consistent with small theoretically predicted differences in equilibrium clumping (Schauble et al. 2006, Hill et al. 2014) and/or acid fractionation (Guo et al. 2009) with the identity of the cation to which the carbonate ion bonds (Figure 3).

Currently, two T- Δ_{47} calibrations stand out as the most rigorously replicated and standardized composite T- $\Delta_{\rm i}$ calibrations available. The CDES-referenced calibration of Petersen et al. (2019) is a compilation and recalculation of existing data [n=132 samples (>1,200 replicate analyses) from 11 laboratories] spanning 4–800°C generated prior to the establishment of I-CDES. The calibration of Anderson et al. (2021) is based on a reanalysis of original materials with tightly controlled precipitation temperatures, standardized using I-CDES best practices, and spanning a temperature range of 0.5–1,100°C with n=91 samples (>1,400 replicates) from 5 laboratories. These two calibrations are offset by 3°C near 25°C and 7°C near 100°C and show a similar temperature dependence as Δ_{47} theoretical equilibrium calculations (Schauble et al. 2006, Hill et al. 2014) (**Figure 3**). Currently, the one existing T- Δ_{638} calibration dataset [6–1,100°C, 51 synthetic carbonates (Yanay et al. 2022)] is rigorously referenced to both CDES and I-CDES, and is consistent in slope with IRMS studies (**Figure 3**). Small offsets in intercept are to be expected as Δ_{638} is not identical to Δ_{47} (**Supplemental Companion 8**).

3.6. Uncertainty in a $T\Delta_{47}$ Estimate

Although uncertainty on a single Δ_{47} analysis is lower than for $\delta^{18}O$ thanks to long Δ_{47} measurement time, typical uncertainties of 0.010% and 0.05%, respectively, correspond to higher

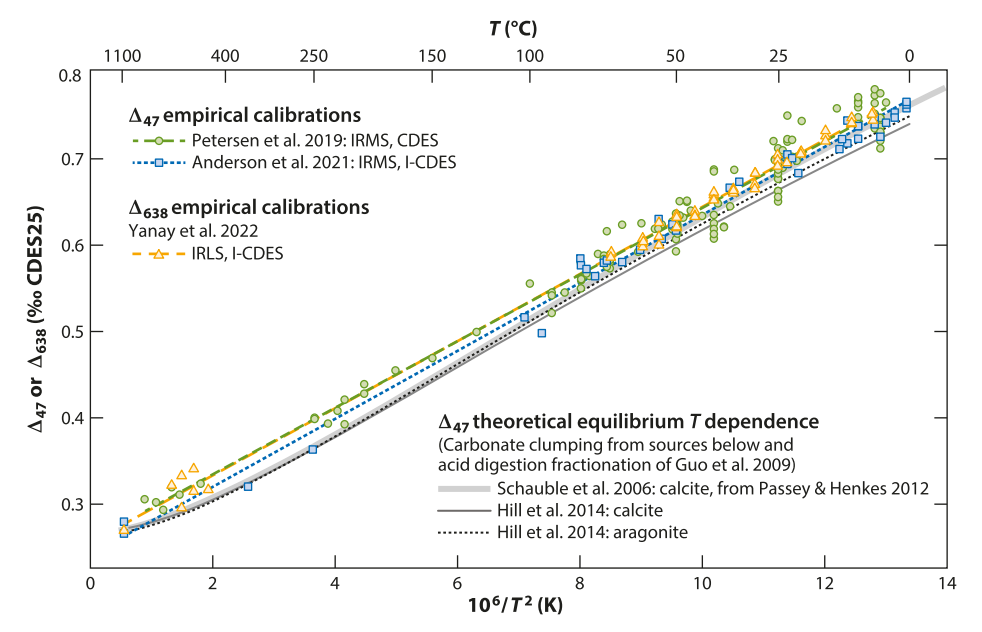


Figure 3

Comparison of theory and recent empirical T calibrations for mass spectrometer (Δ_{47}) and laser spectrometer–based (Δ_{638}) carbonate clumped isotope thermometry. The composite CDES-referenced T- Δ_{47} calibration of Petersen et al. (2019) and I-CDES-referenced calibration of Anderson et al. (2021) are rigorously replicated and standardized. These two calibrations are offset from each other by 3°C near 25°C and 7°C near 100°C and show a similar temperature dependence as the Δ_{47} theoretical equilibrium calculations of Schauble et al. (2006) and Hill et al. (2014) (difference of ~2°C at Earth surface temperatures). The IRLS-based empirical T- Δ_{638} calibration of Yanay et al. (2022), shown referenced to I-CDES, is consistent in slope with Δ_{47} IRMS studies and theory. Small offsets in intercept are to be expected as Δ_{638} is not identical to Δ_{47} (see **Supplemental Companion 8**). See **Supplemental Companion 11** for details. Abbreviations: CDES, carbon dioxide equilibrium scale; I-CDES, Intercarb-carbon dioxide equilibrium scale; IRLS, isotope-ratio laser spectrometer; IRMS, isotope-ratio mass spectrometer; T, temperature.

Supplemental Material >

temperature uncertainties for Δ_{47} thermometry than for $\delta^{18}O$ thermometry due to the relative insensitivity of the Δ_{47} metric to temperature. Carbonate Δ_{47} varies $\sim 0.005\%$ /°C near 25°C, compared to $\sim 0.22\%$ /°C for $\delta^{18}O$. Therefore, Δ_{47} analyses of carbonate sample powders are routinely replicated at least three times [and sometimes more than 20 times for microsample methods (Meckler et al. 2014, Fernandez et al. 2017)] and averaged to reduce uncertainty on Δ_i and resulting $T\Delta_i$.

Uncertainty on the final sample average Δ_{47} value made from analyses of multiple aliquots of sample powder is characterized using the long-term reproducibility [standard deviation (SD)] of replicated carbonate standard analyses, or the SD of replicate sample analyses (i.e., individual acid reactions of carbonate), whichever is larger (**Supplemental Companion 12**). One must propagate this uncertainty, along with error contributions from standardization (ETF) and the empirical temperature calibration, into the ultimate temperature estimate and through any $\delta^{18}O_w$ or other calculations based on $T\Delta_i$. The contribution from $T-\Delta_i$ calibration uncertainty is small compared to the contribution from sample and reference frame measurements (e.g., Petersen et al. 2019, figure 8). Analysts optimize the number of sample versus standard replicates to achieve the lowest uncertainty on final temperatures (e.g., Kocken et al. 2019, Daëron 2021). Various

strategies exist for optimizing sample mass, analysis time, and replication to achieve desirable precision (**Supplemental Companions 7 and 12**). Up to $1-2^{\circ}$ C external precision (2 standard error of the mean) can be achieved with extensive replication (e.g., Petersen et al. 2019). With sufficient reference frame measurements, Δ_i and temperature differences between sample unknowns with similar bulk isotopic compositions that were analyzed together may be more precisely constrained than their absolute Δ_i and temperature values (Daëron 2021).

4. TEMPERATURE AND OTHER CONTROLS ON ISOTOPIC CLUMPING IN NATURAL CARBONATE

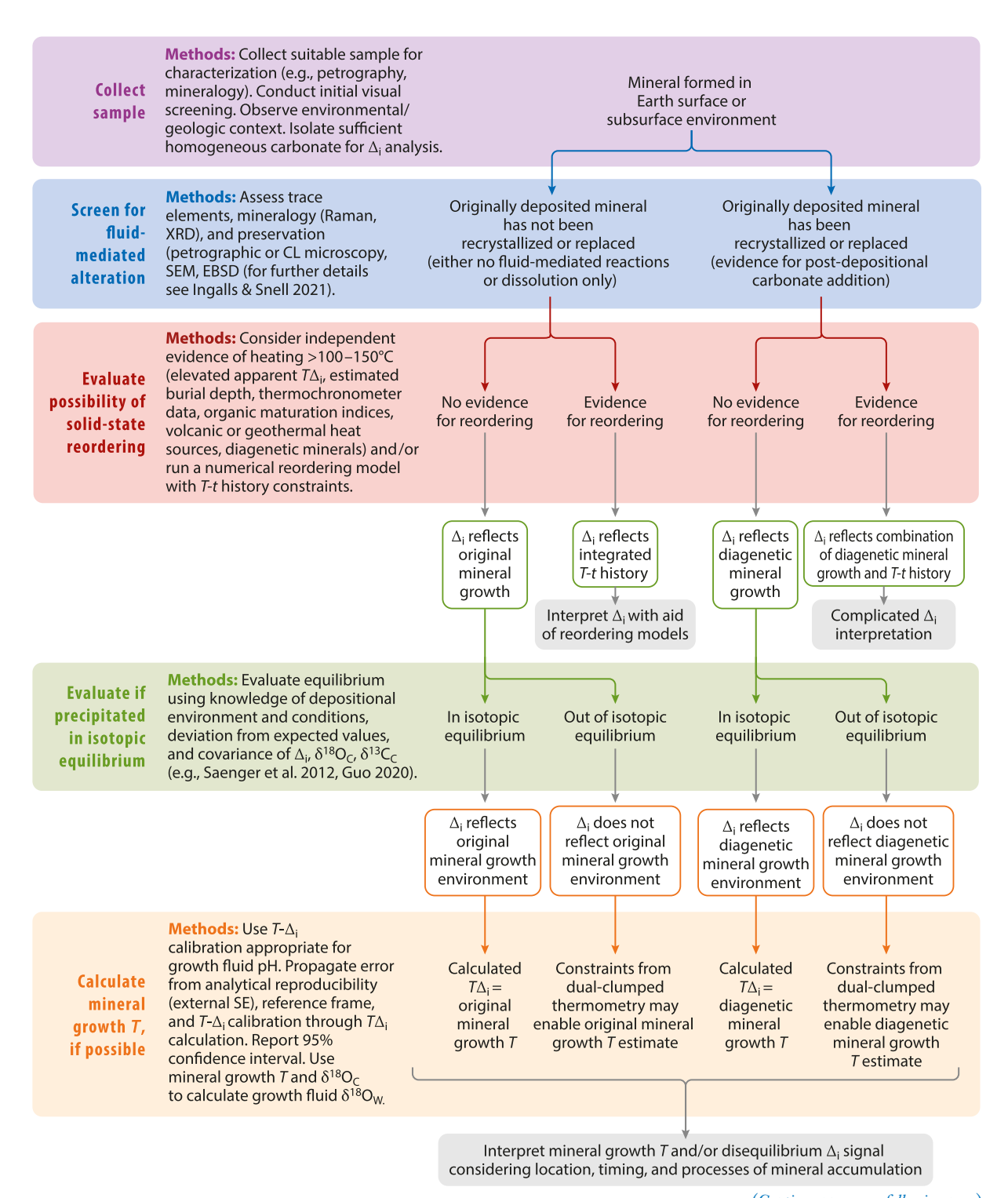
Provided (a) a carbonate precipitated in similar equilibrium (or nonequilibrium) and pH conditions as the known temperature samples used to construct the T- Δ_i calibration, and (b) its isotopic composition and state of ordering has not been post-depositionally altered, depositional temperatures and growth fluid compositions can be reconstructed directly from T- Δ_i relationships described in Section 3.5. Depending on the chosen archive, this reconstruction may represent ancient oceans, lakes, soils, springs, hydrothermal systems, fault zones, and other Earth surface and subsurface environments (Section 5). The following paragraphs describe additional processes affecting Δ_i , apparent $T\Delta_i$ values, and their interpretation (**Figure 4**).

4.1. (Dis)equilibrium Carbonate Precipitation and pH Effects

Clumped isotope equilibrium/disequilibrium and pH effects are governed by processes of the carbonate-water-dissolved inorganic carbon (DIC = $CO_{2(aq)} + HCO_3^- + CO_3^{2-}$) system. Carbonate minerals precipitate out of solution by combining $[CO_3^{2-}]$ with a cation (e.g., Ca^{2+}). The abundance and isotopic composition of $[CO_3^{2-}]$ are determined by carbonate speciation, or the series of reactions that convert gaseous CO_2 to $CO_{2(aq)}/H_2CO_3$ to HCO_3^- to CO_3^{2-} and back again through addition/subtraction of H^+ ions, such that the dominant DIC species varies with pH $[CO_{2(g)} + H_2O \rightleftharpoons H_2CO_{3(aq)} \rightleftharpoons HCO_3^ (aq) + H^+$ $(aq) \rightleftharpoons CO_3^{2-}$ $(aq) + 2 H^+$ (aq)]. This DIC system chemically equilibrates in seconds to minutes, resetting the relative abundances of each carbonate species if one is added/removed such as through carbonate mineral growth (CO_3^{2-} removed) or CO_2 addition/degassing (H_2CO_3 added/removed) (Guo 2020). Isotopic equilibrium, or resetting the relative isotopic compositions of each DIC species through isotopic exchange reactions, takes longer to achieve, in minutes to hours for inorganic systems (Guo 2020), although many biotic systems contain carbonic anhydrase, which dramatically speeds up the exchange process (Uchikawa & Zeebe 2012). Carbonates form in isotopic equilibrium when precipitation rates are slower than DIC isotopic re-equilibration timescales.

T- Δ_i calibrations (Section 3.5) assume equilibrium carbonate precipitation at normal pH (7–9), where the dominant DIC species is HCO₃⁻. Equilibrium clumped isotopic compositions of the DIC species depend on temperature, but at a given temperature fewer clumped isotopologues are found in CO₃²⁻ than in HCO₃⁻ or H₂CO₃ (Hill et al. 2014, Tripati et al. 2015). This means that in extreme pH environments (such as where [CO₃²⁻] is dominant, pH > 9.5), shifts in the chemical and isotopic equilibrium of the H₂O-DIC-CaCO₃ system cause carbonates to follow a different equilibrium T- Δ_i relationship (Tripati et al. 2015, Watkins & Hunt 2015). While such effects may complicate clumped isotope temperature reconstructions (e.g., Sections 5.1 and 5.2), they can also be leveraged to provide new constraints on kinetic isotope effects (KIEs) and processes of the carbonate-DIC-H₂O system (Watkins & Devriendt 2022) (Section 5.4).

Carbonates precipitate out of equilibrium when growth rates are faster than DIC isotopic re-equilibration timescales. Under these conditions, KIEs associated with rapid carbonate precipitation can arise from multiple processes, some of which are biologically mediated. Other



(Caption appears on following page)

Figure 4 (Figure appears on preceding page)

Flowchart to aid in interpretation of measured sample carbonate Δ_i values. A sample carbonate mineral is collected along with observations of the geological/environmental context. Samples, whether formed in Earth surface or subsurface environments, must be screened for fluid-mediated alteration, and the possibility of solid-state reordering must be evaluated. The Δ_i values of minerals unaffected by solid-state reordering may reflect isotopic equilibrium or disequilibrium precipitation. Calculated $T\Delta_i$ values of unaltered samples that precipitated in isotopic equilibrium reflect original growth environment temperatures. For unaltered minerals that precipitated out of isotopic equilibrium, Δ_i values and constraints from dual-clumped isotope thermometry may enable original growth temperature to be calculated. Mineral growth temperature estimates and/or disequilibrium Δ_i signals must be interpreted by considering the location, timing, and processes of mineral accumulation. The flowchart indicates suggested methods to be applied at each step of an investigation including sample collection, evaluation, and interpretation. Abbreviations: CL, cathodoluminescence; EBSD, electron backscatter diffraction; SEM, scanning electron microscopy; T, temperature; t, time; XRD, X-ray diffraction.

processes include mass-dependent diffusive transport of CO₂ through membranes (Thiagarajan et al. 2011), mass-dependent crystal growth reactions (DePaolo 2011), and incomplete isotopic exchange reactions between DIC species and water (e.g., Zeebe & Wolf-Gladrow 2001).

The magnitude of these effects often approaches our analytical uncertainty and can therefore be difficult to detect. Promising work with paired Δ_{47} - Δ_{48} (dual-clumped isotope) measurements can reveal the occurrence of disequilibrium precipitation (Fiebig et al. 2019, 2021; Bajnai et al. 2020; Guo 2020; Swart et al. 2021). Because both Δ_{48} and Δ_{47} are temperature dependent, their values in equilibrium carbonate should follow a paired $\Delta_{i-}T$ relationship predictable by theory. Where observed isotopic compositions deviate from this, the direction of offset can indicate the mechanism at play (e.g., CO_2 degassing produces higher Δ_{48} and lower Δ_{47} ; CO_2 absorption produces the opposite signal). If the magnitude of the offset is small enough, accurate formation temperatures can potentially be reconstructed based on modeled disequilibrium slopes (Bajnai et al. 2020, Guo 2020, Fiebig et al. 2021).

4.2. Post-Depositional Fluid-Mediated and Solid-State Reactions

Following deposition of original carbonate in surface or subsurface environments, conditions during a carbonate's geological lifetime can alter both the bulk isotopic composition and the bonding of heavy isotopes within the carbonate material, overprinting or fully erasing the originally recorded formation temperature and fluid composition. This is ruinous if the desire is to reconstruct past Earth surface conditions but can be leveraged to provide unique constraints on subsurface and diagenetic environments and processes (e.g., Huntington et al. 2011, Dale et al. 2014) (Section 5.3). Often described simply as alteration, post-depositional effects actually include many different processes that can be generally grouped into two categories: fluid mediated and solid state.

Fluid-mediated alteration includes dissolution (loss of original material), as well as overprinting via recrystallization (replacement of dissolved material with new material) and/or secondary growth (addition of new carbonate material on top of unaltered material). Each can occur to a lesser/greater extent within a given sample, altering the original bulk and clumped isotopic compositions to a corresponding lesser/greater degree. Dissolution alone may not affect $T\Delta_i$ very much or at all (O'Hora et al. 2022), whereas addition of, or replacement with, new material will shift $T\Delta_i$, as well as bulk δ^{13} C and δ^{18} O, away from representing conditions of the original depositional environment and toward the diagenetic environment, whether that is hotter or colder than the original environment of precipitation. Fluid-mediated alteration can occur in any environment and at any temperature. Certain carbonate materials may be more prone to this type of alteration due to increased mineral surface area [i.e., micrite (Winkelstern & Lohmann 2016)] or metastability (i.e., aragonite).

Fluid-mediated alteration can be detected using traditional carbonate screening methods such as cathodoluminescence (CL) microscopy and trace element analysis to identify the addition of new material derived from diagenetic fluids, scanning electron microscopy (SEM) to evaluate expected original versus diagenetic mineral fabrics or evidence of dissolution, and Raman spectroscopy and X-ray diffraction (XRD) to detect a change in mineralogy. Crystallographic orientation data from electron backscatter diffraction (EBSD) can indicate preservation or alteration of original mineral fabrics. These and other approaches are summarized in the review by Ingalls & Snell (2021).

Solid-state reactions involve exchange of bonds (reordering) with no gain or loss of volume and no change in the bulk isotopic composition. At temperatures above 100–150°C (Passey & Henkes 2012, Stolper & Eiler 2015, Winkelstern & Lohmann 2016, Hemingway & Henkes 2021), bonds between carbon and oxygen atoms begin to break and reform, altering the number of multiply substituted isotopologues, and effectively resetting the apparent $T\Delta_i$ value gradually toward the (usually higher) temperature of the diagenetic environment. Both the maximum temperature reached and residence time at that temperature (million-year timescales) are important constraints on the extent of Δ_i change via this alteration pathway. Solid-state reactions can occur anywhere that temperatures exceed this threshold but are especially important to consider in geologically older samples that may have been buried deeply and exhumed, or buried more shallowly for millions of years.

Bond reordering cannot be directly detected in the same way as the fluid-mediated processes described above but can be inferred from other information. This may include clumped isotope data for coexisting phases in the sample (e.g., vein calcite crosscutting a dense lacustrine micrite sample) or in the region (e.g., carbonate country rock hosting a hydrothermal calcite vein of interest or from a neighboring unit). Separate knowledge of the thermal history of a sample can rule out (if less than 100°C since deposition) or be used to quantify the extent to which bond reordering may have affected Δ_i . Methods such as vitrinite reflectance, thermochronology of other minerals, and stratigraphic estimates of maximum overburden can be used to estimate maximum burial temperature. Full temperature-time (T-t) histories, if available, can be fed into models to acquire quantitative estimates of the change in Δ_i from the initial value (e.g., Hemingway & Henkes 2021). Because apparent $T\Delta_i$ values elevated by bond reordering may show little to no accompanying change in $\delta^{18}O_C$, bond reordering may manifest as unreasonably high $\delta^{18}O_w$ values and a $T\Delta_i$ and $\delta^{18}O_w$ correlation (Shenton et al. 2015, Jones et al. 2022). Reordering is often discussed as an alternative to fluid-mediated alteration. However, in reality, the conditions in which reordering occurs (high T, subsurface) probably do not occur in the absence of microscale fluid-mediated alteration, although such fine-scale alteration may escape detection even with techniques capable of detecting changes associated with individual micrite grains (i.e., CL, EBSD, SEM).

Some biogenic carbonates originally precipitated as aragonite subsequently may have been converted to calcite through heating and/or dissolution/reprecipitation reactions. Such a change in mineralogy would completely reset Δ_i values, but may occur without much transfer of mass in or out, so it thus falls somewhere between fluid-mediated alteration and bond reordering. However, this and other mineralogy changes (e.g., dolomitization) are easily detected if the original mineralogy is known and differs from the current mineralogy, assessed using Raman spectroscopy or XRD.

4.3. Other Biases

Even in the most ideal precipitation and preservation environments, care must be taken in interpreting reconstructed temperatures with respect to timing of growth and sample heterogeneity. In many biogenic (mollusk, foraminifera, corals) and abiogenic (lake sediments, soils) carbonates, carbonate accumulation can be seasonally biased due to preferable growth conditions occurring in only one season versus another. Heterogeneous carbonate materials, such as a fault-hosted vein made up of multiple generations of diagenetic calcite precipitated from different fluid sources, can provide a wealth of information on depositional conditions through time. However, interpretations may be complicated if these phases occur at too fine a scale to separate physically during sampling. When materials with different bulk and/or clumped isotopic compositions are combined, the Δ_i value of the mixture can be either elevated or reduced relative to the expected linear mixed value (Eiler & Schauble 2004, Defliese et al. 2015b).

5. APPLICATIONS, SCIENCE ADVANCES, AND FUTURE OPPORTUNITIES

5.1. Marine Paleoclimate and Paleoceanography

Marine carbonates have been a reliable source of robust paleoclimate information for decades via oxygen isotope paleothermometry. Unfortunately, this proxy has been limited in reconstructing absolute temperatures deeper into the past by its major weakness—the codependence of temperature estimates on the oxygen isotopic composition of seawater, which is less well constrained further back in time, especially over periods of changing ice volume. This lack of accuracy of the oxygen isotope paleothermometer is often forgotten in the face of its excellent precision ($\sim 0.1\%$, ~ 0.5 °C), leading paleotemperatures to be interpreted with too much confidence.

Clumped isotope paleothermometry in the marine realm defines absolute seawater temperatures in the past. Δ_{47} values in foraminifera (Tripati et al. 2010, Grauel et al. 2013, Peral et al. 2018, Piasecki et al. 2019, Meinicke et al. 2020), mollusks (Eagle et al. 2013a, Henkes et al. 2013, Came et al. 2014), and coccolithophorids (Tripati et al. 2010, Katz et al. 2017) follow the same T- Δ_{47} relationship as synthetic carbonates, eliminating the time and effort needed to define species-specific calibrations. Unlike δ^{18} O and Mg/Ca thermometry, under typical marine conditions, Δ_i -based temperatures are independent of seawater pH, DIC, and carbonate saturation state (Eagle et al. 2013a, Hill et al. 2014, Tang et al. 2014, Watkins & Hunt 2015, Kelson et al. 2017). Despite a larger uncertainty on a single sample temperature (± 1 –2°C) compared to δ^{18} O thermometry, overall uncertainty can be improved through replication (Thiagarajan et al. 2011) and/or through averaging multiple samples per horizon.

Clumped isotope studies quantifying $\delta^{18}O_{seawater}$ in deep time are beginning to answer long-standing questions about secular changes in global $\delta^{18}O_{seawater}$ and the magnitude of ancient global warmth (Finnegan et al. 2011, Cummins et al. 2014, Bergmann et al. 2018, Henkes et al. 2018, Ryb & Eiler 2018, Vickers et al. 2021). Absolute ocean temperatures derived from Δ_{47} are revealing biases in other proxies, such as a hot bias in TEX86-derived temperatures in the Cretaceous (Meyer et al. 2018) and pH-linked cool bias in $\delta^{18}O$ - and Mg/Ca-derived temperatures in the Eocene (Agterhuis et al. 2022).

Sample size reductions are opening up new avenues of paleoceanographic exploration in mollusk-based sclerochronology and foram-based paleoceanography. Both of these fields have historically relied heavily on δ^{18} O paleothermometry, making them highly susceptible to systematically biased temperature estimates caused by poorly constrained δ^{18} O_{seawater} in the past, as described above. Methods combining data from multiple small (100–400 ug) aliquots derived from sequential drilling along the growth axis of a mollusk or picked from sequential horizons in a sediment core can simultaneously create high-resolution δ^{18} O time series and robust, lower-resolution $T\Delta_{47}$ and δ^{18} O_{seawater} time series (Grauel et al. 2013, Caldarescu et al. 2021). Already, high-resolution Δ_{47} sclerochronology has identified increased seasonality and warmth in the Late Cretaceous mid-latitude oceans (de Winter et al. 2021). Expanding this type of work to more past

greenhouse and icehouse time periods could provide valuable additional targets for validation of global climate models (Tierney et al. 2020).

A recent study (Meckler et al. 2022) marks the first step toward building a Δ_i -based curve of absolute seawater temperatures through the Cenozoic to replace the iconic $\delta^{18}O_C$ curve (Zachos et al. 2001). The accompanying $\delta^{18}O_{seawater}$ curve can also be used to estimate global ice volume through time (Leutert et al. 2020, Modestou et al. 2020). Over the next decade, a community goal should be to reproduce this work using more cores in other ocean basins, building a multi-basin stacked temperature record of absolute Δ_i -derived seawater temperatures for the globe.

5.2. Terrestrial Paleoenvironmental Reconstruction

Isotopic compositions of primary carbonates deposited in terrestrial soils, lakes, springs, and caves are among the most widely used geological archives of past environments. However, the environments in which terrestrial carbonates form are complicated. Spatial heterogeneity, seasonality, evaporation, and other factors make ancient $\delta^{18}O_w$ —and therefore temperature—even harder to constrain via $\delta^{18}O$ paleothermometry than in the ocean. Early workers showed the power of clumped isotope data to get around this problem, developing previously impossible environmental temperature and $\delta^{18}O_w$ reconstructions from terrestrial carbonates including ancient pedogenic (soil) carbonates (e.g., Ghosh et al. 2006b, Passey et al. 2010), lake sediments and freshwater mollusks (e.g., Huntington et al. 2010, Dennis et al. 2013, Hren et al. 2013, Lechler et al. 2013), land snails (e.g., Eagle et al. 2013b), and spring (e.g., Hudson et al. 2017, Parrish et al. 2019) and cave deposits (e.g., Affek et al. 2008, Wainer et al. 2011, Kluge & Affek 2012).

Understanding the timing, location, and conditions of mineral growth is key to interpreting the significance of reconstructed temperature and $\delta^{18}O_w$ values, especially in variable terrestrial environments. In soil carbonates, early data suggested that $T\Delta_{47}$ were biased toward summertime soil temperatures far in excess of air temperatures due to preferential warm-season formation and effects of radiative ground heating (Quade et al. 2013, Snell et al. 2013). We now know that radiative heating is limited (Burgener et al. 2019, Gallagher et al. 2019), and rigorously calibrated and reproduced data (see review by Kelson et al. 2020) show pedogenic carbonate accumulation can be biased to different times of the year in different moisture regimes or climatological conditions (Peters et al. 2013, Hough et al. 2014, Burgener et al. 2016, Gallagher & Sheldon 2016, Huth et al. 2019). The time is ripe to develop proxy-system models to rigorously reconstruct the suite of environmental conditions [e.g., mean-annual and seasonal temperatures, precipitation, partial pressure of carbon dioxide (pCO_2)] that best predict the ensemble of observations from a paleosol horizon (e.g., soil carbonate and organic matter geochemistry, $\delta^{18}O_w$, soil texture, paleobotanical data, etc.).

Authigenic lacustrine carbonate (Anderson et al. 2021) and tufa/travertine (Kele et al. 2015) appear to follow recent synthetic T- Δ_{47} calibrations, but such materials (e.g., Huntington et al. 2010, Kato et al. 2019, Li et al. 2021) as well as biogenic or biologically mediated freshwater carbonates (e.g., Huntington et al. 2015, Petryshyn et al. 2015, Wang et al. 2021) may exhibit seasonal, kinetic, and/or biological effects. Better process-based understanding of freshwater carbonate records will be aided by additional modern carbonate studies and observations of Δ_{47} , Δ_{48} , and δ^{18} O in the same samples.

Clumped isotope constraints on the terrestrial paleoenvironment have advanced understanding of the geosphere, atmosphere, biosphere, and their interactions, setting the stage for future discoveries. Examples include contributions to understanding climate dynamics and the evolution of biological habitats with constraints on continental temperatures and hydroclimate (e.g., Affek et al. 2008, Passey et al. 2010, Suarez et al. 2011, Eagle et al. 2013b, Tobin et al. 2014, Hudson

et al. 2017, Zhang et al. 2018, Page et al. 2019, de Winter et al. 2021). Such datasets can also constrain paleotopography and tectonics (e.g., Ghosh et al. 2006b, Huntington et al. 2010, Garzione et al. 2014, Li et al. 2019, Rugenstein et al. 2022). Soil carbonate $T\Delta_{47}$ and $\delta^{18}O_w$ constraints have improved paleo-CO₂ reconstructions (e.g., Ji et al. 2018). Increasingly sophisticated assessment of depositional environment, diagenesis, proxy system, and hydroclimate effects (e.g., Kelson et al. 2020, Ingalls et al. 2020, Song et al. 2022) is key to these and future applications. There is opportunity to combine clumped isotope thermometry with carbonate geochronology and submillennial sampling (e.g., Huth et al. 2020), and to collect complementary observations [e.g., carbonate $\Delta^{17}O$ (Beverly et al. 2021) or clay $\delta^{18}O$ analyses (Kukla et al. 2022)], all of which could be included in proxy-system models. In the next decade, carbonate clumped isotope thermometry could significantly improve atmospheric pCO_2 reconstruction from soils over the Phanerozoic and reconstruct past Earth surface environments to inform predictions of future environmental change.

5.3. Carbonates Precipitated or Altered in the Subsurface: Constraining Diagenesis and Crustal Processes

Understanding of the kinetics of bond reordering at elevated temperature has increased significantly through experimental and modeling studies (e.g., Passey & Henkes 2012, Stolper & Eiler 2015, Brenner et al. 2018, Lloyd et al. 2018, Chen et al. 2019, Hemingway & Henkes 2021) and by studies in natural laboratories (e.g., Henkes et al. 2014, Shenton et al. 2015, Lloyd et al. 2017, Brenner et al. 2021). Open-source reordering and other models (e.g., Stolper et al. 2018) help quantify how burial histories affect isotopic clumping (e.g., Lacroix & Niemi 2019). To date, this knowledge has mostly been used for sample screening purposes, to assess post-depositional alteration of primary carbonates used for Earth surface temperature reconstructions—in some cases upending previous interpretations (e.g., Bristow et al. 2011, Smith & Swart 2022).

The potential to study thermal histories and fluid sources in their own right with carbonate clumped isotope thermometry is just beginning to be realized. Clumped isotope data for carbonates precipitated or altered in the subsurface have placed new constraints on dolomitization and carbonate reservoirs (e.g., Ferry et al. 2011, Murray & Swart 2017, Chang et al. 2020, Hu et al. 2022), ore formation (e.g., del Real et al. 2016, Mering et al. 2018), geothermal processes (Honlet et al. 2018, Lu et al. 2018), fault zones and fluid-structure interactions (e.g., Swanson et al. 2012, Budd et al. 2013, Dennis et al. 2019), and fold-thrust belt evolution (Looser et al. 2021, Hoareau et al. 2021, Sarkar et al. 2021).

Looking ahead, coupling Δ_{47} analysis and burgeoning carbonate U-Pb dating (e.g., Mangenot et al. 2018, Pagel et al. 2018, MacDonald et al. 2019) and mineralogical, petrographic, fluid inclusion, and other geochemical data (e.g., Nooitgedacht et al. 2021) will be key to reconstructing crustal deformation, basin thermal histories, and reaction dynamics in these environments. There is untapped potential to study thermal and fluid evolution relevant to critical elements and minerals (Doran 2022), neotectonics (e.g., Brogi et al. 2020), and paleoseismology. These methods could be used to understand carbon sequestration in geothermal and epithermal environments where it has occurred naturally to inform strategies for long-term, safe sequestration of captured CO₂.

5.4. Constraints on the CaCO₃-DIC-H₂O System

Historically, carbonates precipitated out of chemical and/or isotopic equilibrium were avoided because δ^{18} O (and δ^{13} C) signals could not be properly interpreted. Δ_{47} , and even more so its use in concert with Δ_{48} , opens up the possibility of extracting real temperature signals from these previously inaccessible archives. Biologic effects on δ^{18} O and δ^{13} C displayed by some carbonate-secreting organisms eliminated many species from possible study. In some cases, $T\Delta_{47}$ was immune

to these biases [foraminifera (Section 5.1)], whereas in others, biologic effects were seen in Δ_{47} as well as δ^{18} O and δ^{13} C [corals (Saenger et al. 2012, Spooner et al. 2016)]. Increasingly, patterns in δ^{18} O, Δ_{47} , and Δ_{48} can inform the mechanisms behind biologic effects (Curley et al. 2023). Such insights can both allow reconstruction of original temperature signals in spite of biologic effects and reveal physiological biomineralization processes going on in different organisms relevant to understanding evolution and organism adaptability.

Speleothems are another climate archive that has been heavily leveraged for $\delta^{18}O$ but displayed complicating disequilibrium signals in Δ_{47} due to rapid degassing and rapid precipitation (Affek et al. 2008, Daëron et al. 2011, Wainer et al. 2011, Kluge & Affek 2012; but see Meckler et al. 2015). This valuable climate archive is now back on the table due to Δ_{48} (Bajnai et al. 2020). In the future we may see cave-based Δ_{47} climate records revealing past climate and monsoon dynamics at high temporal resolution, similar to current $\delta^{18}O$ speleothem records. Beyond just speleothems, there is an opportunity to correct for kinetic effects in spring deposits (Falk et al. 2016) and cryogenic carbonates (Kluge et al. 2014, Burgener et al. 2018).

When fluid pH exceeds 9.5 (Tang et al. 2014), Δ_{47} begins to deviate from known T- Δ_i relationships. Better defining of the T- Δ_i relationship at high pH through modeling and experimental studies may expand the possible locations in which clumped isotopes may be applied to include extreme (hydrothermal) environments. Rapid growth rates have also been hypothesized to cause deviations in Δ_{47} (Huyghe et al. 2022). Paired Δ_{47} and Δ_{48} has the potential to investigate KIEs in these and many other settings. Modeling work has complemented experimental studies in this direction (Hill et al. 2014, Guo & Zhou 2019, Guo 2020). This is a rapidly growing area of clumped isotope research, with only a few papers to date. As more labs perfect Δ_{48} measurements, we expect more work in this area and more discoveries.

6. SUMMARY AND OUTLOOK

- 1. Carbonate clumped isotope thermometry is entering the mature phase of proxy development. As a result of sustained community effort, early technological and calibration issues have been largely resolved. The method now routinely achieves absolute temperature estimates with 1–2°C external precision (2 standard error of the mean) for Earth surface temperatures (<40°C), given sufficient replication (of a single sample) or averaging (of multiple samples from the same growth environment).
- 2. Technological advancements, particularly automation of sample preparation, and availability of complete off-the-shelf preparation and analysis systems are making this challenging measurement more routine and available to a wider community. Lessons learned from Δ_{47} analysis are quickly being adapted to Δ_{48} . Recent innovations in laser spectroscopy promise to be a game changer for speed of Δ_{638} analysis, and laser-based analyses of other isotopologues are on the horizon.
- 3. Carbonate clumped isotope thermometry has contributed significantly and broadly to the geosciences, including advances in terrestrial and marine paleoclimatology, tectonics, and low-temperature geochemistry. Applications of this technique to natural systems are underpinned by robust theoretical calculations. The particular power of this thermometer over others is seen in settings where fluid $\delta^{18}O_w$ is not known, or disequilibrium effects arise.
- 4. Improved sample screening approaches to detect diagenesis (experimental and model based) are leading to a higher rate of success in paleoclimate projects and new insights into diagenetic processes occurring during fluid-mediated and solid-state reactions. Future work leveraging the sensitivity of carbonate clumped isotopes to these processes will

- be focused toward tectonic questions, hydrothermal and metamorphic environments, and mineralization processes.
- 5. Smaller sample size requirements are making time-honored paleoceanographic methods possible for clumped isotopes (sclerochronology, long foraminifera-based downcore records). The ability to reconstruct temperatures and δ¹⁸O_w in multiple terrestrial environments will impact knowledge of climate change on land, of particular importance for society. The combination of TΔ_i analysis with other paleoclimate proxies (e.g., pCO₂ proxies, Δ¹⁷O for hydrology) and climate models holds particular power to understand climate processes going forward.
- 6. Paired Δ_{47} and Δ_{48} (or laser-based equivalents) show great promise to better understand disequilibrium precipitation, kinetic effects, and the fundamental geochemistry of the water-carbonate-DIC system. Mechanisms underlying isotope effects seen in biologically derived carbonates may be revealed, with implications for understanding evolution and organism adaptability.
- 7. Although unlikely to ever fully replace traditional stable isotopes due to cost, analysis time, and sensitivity to alteration, we expect clumped isotope analyses to become a required complement to conventional $\delta^{13}C$ and $\delta^{18}O$ studies, enabling workers to assess sample preservation and the state of equilibrium during precipitation and pin down absolute temperatures by removing uncertainty in $\delta^{18}O_w$.

Carbonate clumped isotope geochemistry is rapidly becoming a mainstream tool for paleoclimate, tectonics, and low-temperature biogeochemistry, with great potential to expand into new scientific applications. As sample throughput and reproducibility are increasing, datasets (individual and community built) are growing in size. As the volume of carbonate clumped isotope labs and datasets multiplies, the scientific community will find new ways to apply this versatile method. New patterns will emerge; new areas of research will develop. The clumped community's strength is in its camaraderie, which can be leveraged to tackle grand challenges across all areas of geoscience.

DISCLOSURE STATEMENT

The authors are not aware of any affiliations, memberships, funding, or financial holdings that might be perceived as affecting the objectivity of this review.

ACKNOWLEDGMENTS

The authors are grateful for the clumped isotope community's collegiality, which has enabled many advances and discoveries. We thank members of the community who contributed to a survey on "greatest hit" clumped isotope publications; Andrew Schauer for discussions; and Tyler Kukla, Alex Quizon, Casey Saenger, and Jade Zhang for their feedback on an early version of this paper. We thank two anonymous reviewers for comments that improved the paper. K.W.H. acknowledges support from the University of Washington College of the Environment Endowed Professorship in Earth Systems, and S.V.P. from the Sloan Research Fellowship.

LITERATURE CITED

Affek HP. 2012. Clumped isotope paleothermometry: principles, applications, and challenges. *Paleontol. Soc. Pap.* 18:101–14

Affek HP, Bar-Matthews M, Ayalon A, Matthews A, Eiler JM. 2008. Glacial/interglacial temperature variations in Soreq cave speleothems as recorded by 'clumped isotope' thermometry. *Geochim. Cosmochim. Acta* 72(22):5351–60

- Affek HP, Eiler JM. 2006. Abundance of mass 47 CO₂ in urban air, car exhaust, and human breath. *Geochim. Cosmochim. Acta* 70(1):1–12
- Agterhuis T, Ziegler M, de Winter NJ, Lourens LJ. 2022. Warm deep-sea temperatures across Eocene Thermal Maximum 2 from clumped isotope thermometry. *Commun. Earth Environ.* 3(1):39
- Anderson NT, Kelson JR, Kele S, Daëron M, Bonifacie M, et al. 2021. A unified clumped isotope thermometer calibration (0.5–1,100 C) using carbonate-based standardization. *Geophys. Res. Lett.* 48(7):e2020GL092069
- Bajnai D, Guo W, Spötl C, Coplen TB, Methner K, et al. 2020. Dual clumped isotope thermometry resolves kinetic biases in carbonate formation temperatures. Nat. Commun. 11(1):4005
- Bemis BE, Spero HJ, Bijma J, Lea DW. 1998. Reevaluation of the oxygen isotopic composition of planktonic foraminifera: experimental results and revised paleotemperature equations. *Paleoceanography* 13(2):150–60
- Bergmann KD, Finnegan S, Creel R, Eiler JM, Hughes NC, et al. 2018. A paired apatite and calcite clumped isotope thermometry approach to estimating Cambro-Ordovician seawater temperatures and isotopic composition. *Geochim. Cosmochim. Acta* 224:18–41
- Bernasconi SM, Daëron M, Bergmann KD, Bonifacie M, Meckler AN, et al. 2021. InterCarb: a community effort to improve interlaboratory standardization of the carbonate clumped isotope thermometer using carbonate standards. *Geochem. Geophys. Geosyst.* 22(5):e2020GC009588
- Bernasconi SM, Müller IA, Bergmann KD, Breitenbach SF, Fernandez A, et al. 2018. Reducing uncertainties in carbonate clumped isotope analysis through consistent carbonate-based standardization. *Geochem. Geophys. Geosyst.* 19(9):2895–914
- Beverly EJ, Levin NE, Passey BH, Aron PG, Yarian DA, et al. 2021. Triple oxygen and clumped isotopes in modern soil carbonate along an aridity gradient in the Serengeti, Tanzania. *Earth Planet. Sci. Lett.* 567:116952
- Brenner DC, Passey BH, Holder RM, Viete DR. 2021. Clumped-isotope geothermometry and carbonate U–Pb geochronology of the Alta stock metamorphic aureole, Utah, USA: insights on the kinetics of metamorphism in carbonates. *Geochem. Geophys. Geosyst.* 22(4):e2020GC009238
- Brenner DC, Passey BH, Stolper DA. 2018. Influence of water on clumped-isotope bond reordering kinetics in calcite. *Geochim. Cosmochim. Acta* 224:42–63
- Bristow TF, Bonifacie M, Derkowski A, Eiler JM, Grotzinger JP. 2011. A hydrothermal origin for isotopically anomalous cap dolostone cements from south China. *Nature* 474(7349):68–71
- Brogi A, Liotta D, Capezzuoli E, Matera PF, Kele S, et al. 2020. Travertine deposits constraining transfer zone neotectonics in geothermal areas: an example from the inner Northern Apennines (Bagno Vignoni-Val d'Orcia area, Italy). Geothermics 85:101763
- Budd DA, Frost EL, Huntington KW, Allwardt PF. 2013. Syndepositional deformation features in high-relief carbonate platforms: long-lived conduits for diagenetic fluids. 7. Sediment. Res. 83(1):12–36
- Burgener L, Huntington KW, Hoke GD, Schauer A, Ringham MC, et al. 2016. Variations in soil carbonate formation and seasonal bias over > 4 km of relief in the western Andes (30°S) revealed by clumped isotope thermometry. Earth Planet. Sci. Lett. 441:188–99
- Burgener L, Hyland E, Huntington KW, Kelson JR, Sewall JO. 2019. Revisiting the equable climate problem during the Late Cretaceous greenhouse using paleosol carbonate clumped isotope temperatures from the Campanian of the Western Interior Basin, USA. Palaeogeogr. Palaeoclimatol. Palaeoecol. 516:244–67
- Burgener LK, Huntington KW, Sletten R, Watkins JM, Quade J, Hallet B. 2018. Clumped isotope constraints on equilibrium carbonate formation and kinetic isotope effects in freezing soils. *Geochim. Cosmochim. Acta* 235:402–30
- Caldarescu DE, Sadatzki H, Andersson C, Schäfer P, Fortunato H, Meckler AN. 2021. Clumped isotope thermometry in bivalve shells: a tool for reconstructing seasonal upwelling. Geochim. Cosmochim. Acta 294:174–91
- Came RE, Brand U, Affek HP. 2014. Clumped isotope signatures in modern brachiopod carbonate. Chem. Geol. 377:20–30
- Chang B, Li C, Liu D, Foster I, Tripati A, et al. 2020. Massive formation of early diagenetic dolomite in the Ediacaran ocean: constraints on the "dolomite problem." *PNAS* 117(25):14005–14

- Chen S, Ryb U, Piasecki AM, Lloyd MK, Baker MB, Eiler JM. 2019. Mechanism of solid-state clumped isotope reordering in carbonate minerals from aragonite heating experiments. Geochim. Cosmochim. Acta 258:156–73
- Cummins RC, Finnegan S, Fike DA, Eiler JM, Fischer WW. 2014. Carbonate clumped isotope constraints on Silurian ocean temperature and seawater 8¹⁸O. *Geochim. Cosmochim. Acta* 140:241–58
- Curley AN, Petersen SV, Stewart ME, Guo W. 2023. Biologically driven isotopic fractionations in bivalves: from paleoenvironmental problem to paleophysiology proxy. Biol. Rev. https://doi.org/10.1111/brv. 12940
- Daëron M. 2021. Full propagation of analytical uncertainties in Δ₄₇ measurements. Geochem. Geophys. Geosyst. 22(5):e2020GC009592
- Daëron M, Blamart D, Peral M, Affek HP. 2016. Absolute isotopic abundance ratios and the accuracy of Δ₄₇ measurements. Chem. Geol. 442:83–96
- Daëron M, Guo W, Eiler J, Genty D, Blamart D, et al. 2011. ¹³C¹⁸O clumping in speleothems: observations from natural caves and precipitation experiments. *Geochim. Cosmochim. Acta* 75(12):3303–17
- Dale A, John CM, Mozley PS, Smalley PC, Muggeridge AH. 2014. Time-capsule concretions: unlocking burial diagenetic processes in the Mancos Shale using carbonate clumped isotopes. *Earth Planet. Sci. Lett.* 394:30–37
- de Winter NJ, Müller IA, Kocken IJ, Thibault N, Ullmann CV, et al. 2021. Absolute seasonal temperature estimates from clumped isotopes in bivalve shells suggest warm and variable greenhouse climate. *Commun. Earth Environ.* 2(1):121
- Defliese WF, Hren MT, Lohmann KC. 2015a. Compositional and temperature effects of phosphoric acid fractionation on Δ₄₇ analysis and implications for discrepant calibrations. *Chem. Geol.* 396:51–60
- Defliese WF, Lohmann KC. 2015b. Non-linear mixing effects on mass-47 CO₂ clumped isotope thermometry: patterns and implications. *Rapid Commun. Mass Spectrom*. 29(9):901–9
- del Real PG, Maher K, Kluge T, Bird DK, Brown GE Jr., John CM. 2016. Clumped-isotope thermometry of magnesium carbonates in ultramafic rocks. Geochim. Cosmochim. Acta 193:222–50
- Dennis KJ, Affek HP, Passey BH, Schrag DP, Eiler JM. 2011. Defining an absolute reference frame for 'clumped' isotope studies of CO₂. *Geochim. Cosmochim. Acta* 75(22):7117–31
- Dennis KJ, Cochran JK, Landman NH, Schrag DP. 2013. The climate of the Late Cretaceous: new insights from the application of the carbonate clumped isotope thermometer to Western Interior Seaway macrofossil. Earth Planet. Sci. Lett. 362:51–65
- Dennis KJ, Schrag DP. 2010. Clumped isotope thermometry of carbonatites as an indicator of diagenetic alteration. Geochim. Cosmochim. Acta 74(14):4110–22
- Dennis PF, Myhill DJ, Marca A, Kirk R. 2019. Clumped isotope evidence for episodic, rapid flow of fluids in a mineralized fault system in the Peak District, UK. 7. Geol. Soc. Lond. 176(3):447–61
- DePaolo DJ. 2011. Surface kinetic model for isotopic and trace element fractionation during precipitation of calcite from aqueous solutions. *Geochim. Cosmochim. Acta* 75(4):1039–56
- Doran AL. 2022. Tracking ore fluid evolution using clumped C–O isotopes. Nat. Rev. Earth Environ. 3(4):223
- Eagle RA, Eiler JM, Tripati AK, Ries JB, Freitas PS, et al. 2013a. The influence of temperature and seawater carbonate saturation state on ¹³C–¹⁸O bond ordering in bivalve mollusks. *Biogeosciences* 10(7):4591–606
- Eagle RA, Risi C, Mitchell JL, Eiler JM, Seibt U, et al. 2013b. High regional climate sensitivity over continental China constrained by glacial-recent changes in temperature and the hydrological cycle. PNAS 110(22):8813–18
- Eiler JM. 2007. "Clumped-isotope" geochemistry—the study of naturally-occurring, multiply-substituted isotopologues. *Earth Planet. Sci. Lett.* 262(3–4):309–27
- Eiler JM. 2011. Paleoclimate reconstruction using carbonate clumped isotope thermometry. *Quat. Sci. Rev.* 30(25–26):3575–88
- Eiler JM. 2013. The isotopic anatomies of molecules and minerals. Annu. Rev. Earth Planet. Sci. 41:411-41
- Eiler JM, Schauble E. 2004. ¹⁸O¹³C¹⁶O in Earth's atmosphere. *Geochim. Cosmochim. Acta* 68(23):4767–77
- EL-Shenawy MI, Kim ST. 2019. Disordering of $^{13}C^{18}O$ bonds in CO₂ gas over a heated quartz surface at 50–1100°C: insights into the abundance of mass 47 (Δ_{47}) in CO₂ gas at thermodynamic equilibrium. *Chem. Geol.* 524:213–27

- Epstein S, Buchsbaum R, Lowenstam H, Urey HC. 1951. Carbonate-water isotopic temperature scale. Geol. Soc. Am. Bull. 62(4):417–26
- Falk ES, Guo W, Paukert AN, Matter JM, Mervine EM, Kelemen PB. 2016. Controls on the stable isotope compositions of travertine from hyperalkaline springs in Oman: insights from clumped isotope measurements. Geochim. Cosmochim. Acta 192:1–28
- Fernandez A, Müller IA, Rodríguez-Sanz L, van Dijk J, Looser N, Bernasconi SM. 2017. A reassessment of the precision of carbonate clumped isotope measurements: implications for calibrations and paleoclimate reconstructions. Geochem. Geophys. Geosyst. 18(12):4375–86
- Ferry JM, Passey BH, Vasconcelos C, Eiler JM. 2011. Formation of dolomite at 40–80°C in the Latemar carbonate buildup, Dolomites, Italy, from clumped isotope thermometry. *Geology* 39(6):571–74
- Fiebig J, Bajnai D, Löffler N, Methner K, Krsnik E, et al. 2019. Combined high-precision Δ_{48} and Δ_{47} analysis of carbonates. *Chem. Geol.* 522:186–91
- Fiebig J, Daëron M, Bernecker M, Guo W, Schneider G, et al. 2021. Calibration of the dual clumped isotope thermometer for carbonates. Geochim. Cosmochim. Acta 312:235–56
- Finnegan S, Bergmann K, Eiler JM, Jones DS, Fike DA, et al. 2011. The magnitude and duration of Late Ordovician–Early Silurian glaciation. *Science* 331(6019):903–6
- Gallagher TM, Hren M, Sheldon ND. 2019. The effect of soil temperature seasonality on climate reconstructions from paleosols. Am. J. Sci. 319(7):549–81
- Gallagher TM, Sheldon ND. 2016. Combining soil water balance and clumped isotopes to understand the nature and timing of pedogenic carbonate formation. *Chem. Geol.* 435:79–91
- Garzione CN, Auerbach DJ, Smith JJS, Rosario JJ, Passey BH, et al. 2014. Clumped isotope evidence for diachronous surface cooling of the Altiplano and pulsed surface uplift of the Central Andes. Earth Planet. Sci. Lett. 393:173–81
- Ghosh P, Adkins J, Affek H, Balta B, Guo W, et al. 2006a. ¹³C–¹⁸O bonds in carbonate minerals: a new kind of paleothermometer. *Geochim. Cosmochim. Acta* 70(6):1439–56
- Ghosh P, Garzione CN, Eiler JM. 2006b. Rapid uplift of the altiplano revealed through ¹³C–¹⁸O bonds in paleosol carbonates. *Science* 311:511–15
- Grauel AL, Schmid TW, Hu B, Bergami C, Capotondi L, et al. 2013. Calibration and application of the 'clumped isotope' thermometer to foraminifera for high-resolution climate reconstructions. Geochim. Cosmochim. Acta 108:125–40
- Grossman EL, Ku TL. 1986. Oxygen and carbon isotope fractionation in biogenic aragonite: temperature effects. Chem. Geol. Isotope Geosci. Sect. 59:59–74
- Guo W. 2020. Kinetic clumped isotope fractionation in the DIC-H₂O-CO₂ system: patterns, controls, and implications. Geochim. Cosmochim. Acta 268:230–57
- Guo W, Mosenfelder JL, Goddard WA III, Eiler JM. 2009. Isotopic fractionations associated with phosphoric acid digestion of carbonate minerals: insights from first-principles theoretical modeling and clumped isotope measurements. Geochim. Cosmochim. Acta 73(24):7203–25
- Guo W, Zhou C. 2019. Patterns and controls of disequilibrium isotope effects in speleothems: insights from an isotope-enabled diffusion-reaction model and implications for quantitative thermometry. Geochim. Cosmochim. Acta 267:196–226
- He B, Olack GA, Colman AS. 2012. Pressure baseline correction and high-precision CO₂ clumped-isotope (Δ₄₇) measurements in bellows and micro-volume modes. *Rapid Commun. Mass Spectrom.* 26(24):2837–53
- Hemingway JD, Henkes GA. 2021. A disordered kinetic model for clumped isotope bond reordering in carbonates. *Earth Planet. Sci. Lett.* 566:116962
- Henkes GA, Passey BH, Grossman EL, Shenton BJ, Pérez-Huerta A, Yancey TE. 2014. Temperature limits for preservation of primary calcite clumped isotope paleotemperatures. Geochim. Cosmochim. Acta 139:362–82
- Henkes GA, Passey BH, Grossman EL, Shenton BJ, Yancey TE, Pérez-Huerta A. 2018. Temperature evolution and the oxygen isotope composition of Phanerozoic oceans from carbonate clumped isotope thermometry. Earth Planet. Sci. Lett. 490:40–50
- Henkes GA, Passey BH, Wanamaker AD Jr., Grossman EL, Ambrose WG Jr., Carroll ML. 2013. Carbonate clumped isotope compositions of modern marine mollusk and brachiopod shells. Geochim. Cosmochim. Acta 106:307–25

- Hill PS, Tripati AK, Schauble EA. 2014. Theoretical constraints on the effects of pH, salinity, and temperature on clumped isotope signatures of dissolved inorganic carbon species and precipitating carbonate minerals. Geochim. Cosmochim. Acta 125:610–52
- Hoareau G, Crognier N, Lacroix B, Aubourg C, Roberts NM, et al. 2021. Combination of Δ₄₇ and U-Pb dating in tectonic calcite veins unravel the last pulses related to the Pyrenean Shortening (Spain). Earth Planet. Sci. Lett. 553:116636
- Honlet R, Gasparrini M, Muchez P, Swennen R, John CM. 2018. A new approach to geobarometry by combining fluid inclusion and clumped isotope thermometry in hydrothermal carbonates. *Terra Nova* 30(3):199–206
- Hough BG, Fan M, Passey BH. 2014. Calibration of the clumped isotope geothermometer in soil carbonate in Wyoming and Nebraska, USA: implications for paleoelevation and paleoclimate reconstruction. Earth Planet. Sci. Lett. 391:110–20
- Hren MT, Sheldon ND, Grimes ST, Collinson ME, Hooker JJ, et al. 2013. Terrestrial cooling in Northern Europe during the Eocene–Oligocene transition. *PNAS* 110(19):7562–67
- Hu X, Müller IA, Zhao A, Ziegler M, Chen Q, et al. 2022. Clumped isotope thermometry reveals diagenetic origin of the dolomite layer within late Ordovician black shale of the Guanyinqiao Bed (SW China). Chem. Geol. 588:120641
- Hudson AM, Quade J, Ali G, Boyle D, Bassett S, et al. 2017. Stable C, O and clumped isotope systematics and ¹⁴C geochronology of carbonates from the Quaternary Chewaucan closed-basin lake system, Great Basin, USA: implications for paleoenvironmental reconstructions using carbonates. *Geochim. Cosmochim.* Acta 212:274–302
- Huntington KW, Budd DA, Wernicke BP, Eiler JM. 2011. Use of clumped-isotope thermometry to constrain the crystallization temperature of diagenetic calcite. *J. Sediment. Res.* 81(9):656–69
- Huntington KW, Eiler JM, Affek HP, Guo W, Bonifacie M, et al. 2009. Methods and limitations of 'clumped' CO₂ isotope (Δ₄₇) analysis by gas-source isotope ratio mass spectrometry. J. Mass Spectrom. 44(9):1318– 29
- Huntington KW, Lechler AR. 2015. Carbonate clumped isotope thermometry in continental tectonics. Tectonophysics 647–48:1–20
- Huntington KW, Saylor J, Quade J, Hudson AM. 2015. High late Miocene–Pliocene elevation of the Zhada Basin, southwestern Tibetan Plateau, from carbonate clumped isotope thermometry. Bulletin 127(1–2):181–99
- Huntington KW, Wernicke BP, Eiler JM. 2010. Influence of climate change and uplift on Colorado Plateau paleotemperatures from carbonate clumped isotope thermometry. *Tectonics* 29(3):TC3005
- Huth TE, Cerling TE, Marchetti DW, Bowling DR, Ellwein AL, et al. 2020. Laminated soil carbonate rinds as a paleoclimate archive of the Colorado Plateau. *Geochim. Cosmochim. Acta* 282:227–44
- Huth TE, Cerling TE, Marchetti DW, Bowling DR, Ellwein AL, Passey BH. 2019. Seasonal bias in soil carbonate formation and its implications for interpreting high-resolution paleoarchives: evidence from southern Utah. 7. Geophys. Res. Biogeosci. 124(3):616–32
- Huyghe D, Daëron M, de Rafelis M, Blamart D, Sébilo M, et al. 2022. Clumped isotopes in modern marine bivalves. Geochim. Cosmochim. Acta 316:41–58
- Ingalls M, Frantz CM, Snell KE, Trower EJ. 2020. Carbonate facies-specific stable isotope data record climate, hydrology, and microbial communities in Great Salt Lake, UT. Geobiology 18(5):566–93
- Ingalls M, Snell KE. 2021. Tools for comprehensive assessment of fluid-mediated and solid-state alteration of carbonates used to reconstruct ancient elevation and environments. Front. Earth Sci. 9:623982
- Ji S, Nie J, Lechler A, Huntington KW, Heitmann EO, Breecker DO. 2018. A symmetrical CO₂ peak and asymmetrical climate change during the middle Miocene. Earth Planet. Sci. Lett. 499:134–44
- John CM, Bowen D. 2016. Community software for challenging isotope analysis: first applications of 'Easotope' to clumped isotopes. Rapid Commun. Mass Spectrom. 30(21):2285–300
- Jones MM, Petersen SV, Curley AN. 2022. A tropically hot mid-Cretaceous North American Western Interior Seaway. Geology 50(8):954–58
- Kato H, Amekawa S, Kano A, Mori T, Kuwahara Y, Quade J. 2019. Seasonal temperature changes obtained from carbonate clumped isotopes of annually laminated tufas from Japan: discrepancy between natural and synthetic calcites. *Geochim. Cosmochim. Acta* 244:548–64

- Katz A, Bonifacie M, Hermoso M, Cartigny P, Calmels D. 2017. Laboratory-grown coccoliths exhibit no vital effect in clumped isotope (Δ₄₇) composition on a range of geologically relevant temperatures. Geochim. Cosmochim. Acta 208:335–53
- Kele S, Breitenbach SF, Capezzuoli E, Meckler AN, Ziegler M, et al. 2015. Temperature dependence of oxygen- and clumped isotope fractionation in carbonates: a study of travertines and tufas in the 6–95°C temperature range. Geochim. Cosmochim. Acta 168:172–92
- Kelson JR, Huntington KW, Breecker DO, Burgener LK, Gallagher T, et al. 2020. A proxy for all seasons? A synthesis of clumped isotope data from Holocene soil carbonates. Quat. Sci. Rev. 234:106259
- Kelson JR, Huntington KW, Schauer AJ, Saenger C, Lechler AR. 2017. Toward a universal carbonate clumped isotope calibration: Diverse synthesis and preparatory methods suggest a single temperature relationship. *Geochim. Cosmochim. Acta* 197:104–31
- Kim ST, O'Neil JR. 1997. Temperature dependence of ¹⁸O. Geochim. Cosmochim. Acta 61:34613475
- Kim ST, O'Neil JR, Hillaire-Marcel C, Mucci A. 2007. Oxygen isotope fractionation between synthetic aragonite and water: influence of temperature and Mg²⁺ concentration. Geochim. Cosmochim. Acta 71(19):4704–15
- Kluge T, Affek HP. 2012. Quantifying kinetic fractionation in Bunker Cave speleothems using Δ_{47} . Quat. Sci. Rev. 49:82–94
- Kluge T, Affek HP, Zhang YG, Dublyansky Y, Spötl C, et al. 2014. Clumped isotope thermometry of cryogenic cave carbonates. *Geochim. Cosmochim. Acta* 126:541–54
- Kocken IJ, Müller IA, Ziegler M. 2019. Optimizing the use of carbonate standards to minimize uncertainties in clumped isotope data. Geochem. Geophys. Geosyst. 20(11):5565–77
- Kukla T, Rugenstein JKC, Ibarra DE, Winnick MJ, Strömberg CA, Chamberlain CP. 2022. Drier winters drove Cenozoic open habitat expansion in North America. AGU Adv. 3(2):e2021AV000566
- Lacroix B, Niemi NA. 2019. Investigating the effect of burial histories on the clumped isotope thermometer: an example from the Green River and Washakie basins, Wyoming. Geochim. Cosmochim. Acta 247:40–58
- Lechler AR, Niemi NA, Hren MT, Lohmann KC. 2013. Paleoelevation estimates for the northern and central proto–Basin and Range from carbonate clumped isotope thermometry. *Tectonics* 32(3):295–316
- Leutert TJ, Auderset A, Martínez-García A, Modestou S, Meckler AN. 2020. Coupled Southern Ocean cooling and Antarctic ice sheet expansion during the middle Miocene. *Nat. Geosci.* 13(9):634–39
- Li H, Liu X, Arnold A, Elliott B, Flores R, et al. 2021. Mass 47 clumped isotope signatures in modern lacustrine authigenic carbonates in Western China and other regions and implications for paleotemperature and paleoelevation reconstructions. Earth Planet. Sci. Lett. 562:116840
- Li L, Fan M, Davila N, Jesmok G, Mitsunaga B, et al. 2019. Carbonate stable and clumped isotopic evidence for late Eocene moderate to high elevation of the east-central Tibetan Plateau and its geodynamic implications. Geol. Soc. Am. Bull. 131(5–6):831–44
- Lloyd MK, Eiler JM, Nabelek PI. 2017. Clumped isotope thermometry of calcite and dolomite in a contact metamorphic environment. Geochim. Cosmochim. Acta 197:323–44
- Lloyd MK, Ryb U, Eiler JM. 2018. Experimental calibration of clumped isotope reordering in dolomite. Geochim. Cosmochim. Acta 242:1–20
- Looser N, Madritsch H, Guillong M, Laurent O, Wohlwend S, Bernasconi SM. 2021. Absolute age and temperature constraints on deformation along the basal Décollement of the Jura fold-and-thrust belt from carbonate U-Pb dating and clumped isotopes. *Tectonics* 40:e2020TC006439
- Lu YC, Song SR, Taguchi S, Wang PL, Yeh EC, et al. 2018. Evolution of hot fluids in the Chingshui geothermal field inferred from crystal morphology and geochemical vein data. *Geothermics* 74:305–18
- Ma Q, Sheng W, Yongchun T. 2008. Formation and abundance of doubly-substituted methane isotopologues (¹³CH₃D) in natural gas systems. Geochim. Cosmochim. Acta 72(22):5446–56
- MacDonald JM, Faithfull JW, Roberts NMW, Davies AJ, Holdsworth CM, et al. 2019. Clumped-isotope palaeothermometry and LA-ICP-MS U-Pb dating of lava-pile hydrothermal calcite veins. *Contrib. Mineral. Petrol.* 174(7):63
- Mangenot X, Gasparrini M, Gerdes A, Bonifacie M, Rouchon V. 2018. An emerging thermochronometer for carbonate-bearing rocks: Δ₄₇/(U-Pb). Geology 46(12):1067–70
- McCrea JM. 1950. On the isotopic chemistry of carbonates and a paleotemperature scale. *J. Chem. Phys.* 18(6):849–57

- Meckler AN, Affolter S, Dublyansky YV, Krüger Y, Vogel N, et al. 2015. Glacial-interglacial temperature change in the tropical West Pacific: a comparison of stalagmite-based paleo-thermometers. Quat. Sci. Rev. 127:90–116
- Meckler AN, Sexton PF, Piasecki AM, Leutert TJ, Marquardt J, et al. 2022. Cenozoic evolution of deep ocean temperature from clumped isotope thermometry. *Science* 377(6601):86–90
- Meckler AN, Ziegler M, Millán MI, Breitenbach SF, Bernasconi SM. 2014. Long-term performance of the Kiel carbonate device with a new correction scheme for clumped isotope measurements. *Rapid Commun. Mass Spectrom.* 28(15):1705–15
- Meinicke N, Ho SL, Hannisdal B, Nürnberg D, Tripati A, et al. 2020. A robust calibration of the clumped isotopes to temperature relationship for foraminifers. *Geochim. Cosmochim. Acta* 270:160–83
- Mering JA, Barker SL, Huntington KW, Simmons S, Dipple G, et al. 2018. Taking the temperature of hydrothermal ore deposits using clumped isotope thermometry. Econ. Geol. 113(8):1671–78
- Meyer KW, Petersen SV, Lohmann KC, Winkelstern IZ. 2018. Climate of the Late Cretaceous North American Gulf and Atlantic Coasts. *Cretaceous Res.* 89:160–73
- Modestou SE, Leutert TJ, Fernandez A, Lear CH, Meckler AN. 2020. Warm middle Miocene Indian Ocean bottom water temperatures: comparison of clumped isotope and Mg/Ca-based estimates. *Paleoceanogr: Paleoclimatol.* 35(11):e2020PA003927
- Müller IA, Fernandez A, Radke J, van Dijk J, Bowen D, et al. 2017. Carbonate clumped isotope analyses with the long-integration dual-inlet (LIDI) workflow: scratching at the lower sample weight boundaries. *Rapid Commun. Mass Spectrom.* 31(12):1057–66
- Murray ST, Swart PK. 2017. Evaluating formation fluid models and calibrations using clumped isotope paleothermometry on Bahamian dolomites. *Geochim. Cosmochim. Acta* 206:73–93
- Nooitgedacht CW, van der Lubbe HJL, De Graaf S, Ziegler M, Staudigel PT, Reijmer JJG. 2021. Restricted internal oxygen isotope exchange in calcite veins: constraints from fluid inclusion and clumped isotopederived temperatures. *Geochim. Cosmochim. Acta* 297:24–39
- O'Hora HE, Petersen SV, Vellekoop J, Jones MM, Scholz SR. 2022. Clumped-isotope-derived climate trends leading up to the end-Cretaceous mass extinction in northwest Europe. Clim. Past 18:1963–82
- Page M, Licht A, Dupont-Nivet G, Meijer N, Barbolini N, et al. 2019. Synchronous cooling and decline in monsoonal rainfall in northeastern Tibet during the fall into the Oligocene icehouse. Geology 47(3):203– 6
- Pagel M, Bonifacie M, Schneider DA, Gautheron C, Brigaud B, et al. 2018. Improving paleohydrological and diagenetic reconstructions in calcite veins and breccia of a sedimentary basin by combining Δ₄₇ temperature, δ¹⁸O_{water} and U-Pb age. Chem. Geol. 481:1–17
- Parrish JT, Hyland EG, Chan MA, Hasiotis ST. 2019. Stable and clumped isotopes in desert carbonate spring and lake deposits reveal palaeohydrology: a case study of the Lower Jurassic Navajo Sandstone, southwestern USA. Sedimentology 66(1):32–52
- Passey BH, Henkes GA. 2012. Carbonate clumped isotope bond reordering and geospeedometry. Earth Planet. Sci. Lett. 351:223–36
- Passey BH, Levin NE, Cerling TE, Brown FH, Eiler JM. 2010. High-temperature environments of human evolution in East Africa based on bond ordering in paleosol carbonates. *PNAS* 107(25):11245–49
- Peral M, Daëron M, Blamart D, Bassinot F, Dewilde F, et al. 2018. Updated calibration of the clumped isotope thermometer in planktonic and benthic foraminifera. *Geochim. Cosmochim. Acta* 239:1–16
- Peters NA, Huntington KW, Hoke GD. 2013. Hot or not? Impact of seasonally variable soil carbonate formation on paleotemperature and O-isotope records from clumped isotope thermometry. Earth Planet. Sci. Lett. 361:208–18
- Petersen SV, Defliese WF, Saenger C, Daëron M, Huntington KW, et al. 2019. Effects of improved ¹⁷O correction on interlaboratory agreement in clumped isotope calibrations, estimates of mineral-specific offsets, and temperature dependence of acid digestion fractionation. *Geochem. Geophys. Geosyst.* 20(7):3495–519
- Petryshyn VA, Lim D, Laval BL, Brady A, Slater G, Tripati AK. 2015. Reconstruction of limnology and microbialite formation conditions from carbonate clumped isotope thermometry. *Geobiology* 13(1):53–67

- Piasecki A, Bernasconi SM, Grauel AL, Hannisdal B, Ho SL, et al. 2019. Application of clumped isotope thermometry to benthic foraminifera. *Geochem. Geophys. Geosyst.* 20(4):2082–90
- Piasecki A, Sessions A, Peterson B, Eiler J. 2016. Prediction of equilibrium distributions of isotopologues for methane, ethane and propane using density functional theory. Geochim. Cosmochim. Acta 190:1–12
- Prokhorov I, Kluge T, Janssen C. 2019. Laser absorption spectroscopy of rare and doubly substituted carbon dioxide isotopologues. Anal. Chem. 91(24):15491–99
- Quade J, Eiler J, Daëron M, Achyuthan H. 2013. The clumped isotope geothermometer in soil and paleosol carbonate. Geochim. Cosmochim. Acta 105:92–107
- Rugenstein JKC, Methner K, Kukla T, Mulch A, Lüdecke T, et al. 2022. Clumped isotope constraints on warming and precipitation seasonality in Mongolia following Altai uplift. Am. 7. Sci. 322(1):28–54
- Ryb U, Eiler JM. 2018. Oxygen isotope composition of the Phanerozoic ocean and a possible solution to the dolomite problem. PNAS 115(26):6602–7
- Saenger C, Affek HP, Felis T, Thiagarajan N, Lough JM, Holcomb M. 2012. Carbonate clumped isotope variability in shallow water corals: temperature dependence and growth-related vital effects. Geochim. Cosmochim. Acta 99:224–42
- Saenger CP, Schauer AJ, Heitmann EO, Huntington KW, Steig EJ. 2021. How ¹⁷O excess in clumped isotope reference-frame materials and ETH standards affects reconstructed temperature. Chem. Geol. 563:120059
- Sarkar DP, Ando JI, Kano A, Kato H, Ghosh G, Das K. 2021. Carbonate clumped isotope thermometry of fault rocks and its possibilities: tectonic implications from calcites within Himalayan Frontal Fold-Thrust Belt. Prog. Earth Planet. Sci. 8(1):42
- Schauble EA, Ghosh P, Eiler JM. 2006. Preferential formation of ¹³C-¹⁸O bonds in carbonate minerals, estimated using first-principles lattice dynamics. *Geochim. Cosmochim. Acta* 70(10):2510-29
- Schauer AJ, Kelson J, Saenger C, Huntington KW. 2016. Choice of ¹⁷O correction affects clumped isotope (Δ₄₇) values of CO₂ measured with mass spectrometry. *Rapid Commun. Mass Spectrom.* 30(24):2607–16
- Schmid TW, Bernasconi SM. 2010. An automated method for 'clumped-isotope' measurements on small carbonate samples. *Rapid Commun. Mass Spectrom.* 24(14):1955–63
- Sharp Z. 2017. Principles of Stable Isotope Geochemistry. Upper Saddle River, NJ: Prentice Hall. 2nd ed.
- Shenton BJ, Grossman EL, Passey BH, Henkes GA, Becker TP, et al. 2015. Clumped isotope thermometry in deeply buried sedimentary carbonates: the effects of bond reordering and re-crystallization. Geol. Soc. Am. Bull. 127:1036–51
- Smith ME, Swart PK. 2022. The influence of diagenesis on carbon and oxygen isotope values in shallow water carbonates from the Atlantic and Pacific: implications for the interpretation of the global carbon cycle. Sediment. Geol. 434:106147
- Snell KE, Thrasher BL, Eiler JM, Koch PL, Sloan LC, Tabor NJ. 2013. Hot summers in the Bighorn Basin during the early Paleogene. Geology 41(1):55–58
- Song B, Zhang K, Farnsworth A, Ji J, Algeo TJ, et al. 2022. Application of ostracod-based carbonate clumpedisotope thermometry to paleo-elevation reconstruction in a hydrologically complex setting: a case study from the northern Tibetan Plateau. *Gondwana Res.* 107:73–83
- Spencer C, Kim ST. 2015. Carbonate clumped isotope paleothermometry: a review of recent advances in CO₂ gas evolution, purification, measurement and standardization techniques. *Geosci.* 7, 19(2):357–74
- Spooner PT, Guo W, Robinson LF, Thiagarajan N, Hendry KR, et al. 2016. Clumped isotope composition of cold-water corals: a role for vital effects? Geochim. Cosmochim. Acta 179:123–41
- Stolper DA, Eiler JM. 2015. The kinetics of solid-state isotope-exchange reactions for clumped isotopes: a study of inorganic calcites and apatites from natural and experimental samples. *Am. J. Sci.* 315(5):363–411
- Stolper DA, Eiler JM, Higgins JA. 2018. Modeling the effects of diagenesis on carbonate clumped-isotope values in deep- and shallow-water settings. Geochim. Cosmochim. Acta 227:264–91
- Stolper DA, Sessions AL, Ferreira AA, Neto ES, Schimmelmann A, et al. 2014. Combined ¹³C–D and D–D clumping in methane: methods and preliminary results. *Geochim. Cosmochim. Acta* 126:169–91
- Suarez MB, Passey BH, Kaakinen A. 2011. Paleosol carbonate multiple isotopologue signature of active East Asian summer monsoons during the late Miocene and Pliocene. *Geology* 39(12):1151–54

- Swanson EM, Wernicke BP, Eiler JM, Losh S. 2012. Temperatures and fluids on faults based on carbonate clumped–isotope thermometry. Am. 7. Sci. 312(1):1–21
- Swart PK, Burns SJ, Leder JJ. 1991. Fractionation of the stable isotopes of oxygen and carbon in carbon dioxide during the reaction of calcite with phosphoric acid as a function of temperature and technique. Chem. Geol. Isotope Geosci. Sect. 86(2):89–96
- Swart PK, Lu C, Moore EW, Smith ME, Murray ST, Staudigel PT. 2021. A calibration equation between Δ₄₈ values of carbonate and temperature. *Rapid Commun. Mass Spectrom.* 35(17):e9147
- Tang J, Dietzel M, Fernandez A, Tripati AK, Rosenheim BE. 2014. Evaluation of kinetic effects on clumped isotope fractionation (Δ47) during inorganic calcite precipitation. Geochim. Cosmochim. Acta 134:120–36
- Thiagarajan N, Adkins J, Eiler J. 2011. Carbonate clumped isotope thermometry of deep-sea corals and implications for vital effects. *Geochim. Cosmochim. Acta* 75(16):4416–25
- Tierney JE, Poulsen CJ, Montañez IP, Bhattacharya T, Feng R, et al. 2020. Past climates inform our future. Science 370(6517):eaay3701
- Tobin TS, Wilson GP, Eiler JM, Hartman JH. 2014. Environmental change across a terrestrial Cretaceous-Paleogene boundary section in eastern Montana, USA, constrained by carbonate clumped isotope paleothermometry. *Geology* 42(4):351–54
- Tripati AK, Eagle RA, Thiagarajan N, Gagnon AC, Bauch H, et al. 2010. ¹³C–¹⁸O isotope signatures and 'clumped isotope' thermometry in foraminifera and coccoliths. *Geochim. Cosmochim. Acta* 74(20):5697–717
- Tripati AK, Hill PS, Eagle RA, Mosenfelder JL, Tang J, et al. 2015. Beyond temperature: clumped isotope signatures in dissolved inorganic carbon species and the influence of solution chemistry on carbonate mineral composition. Geochim. Cosmochim. Acta 166:344–71
- Uchikawa J, Zeebe RE. 2012. The effect of carbonic anhydrase on the kinetics and equilibrium of the oxygen isotope exchange in the CO_2 – H_2O system: implications for $\delta_{18}O$ vital effects in biogenic carbonates. *Geochim. Cosmochim. Acta* 95:15–34
- Vickers ML, Bernasconi SM, Ullmann CV, Lode S, Looser N, et al. 2021. Marine temperatures underestimated for past greenhouse climate. Sci. Rep. 11(1):19109
- Wainer K, Genty D, Blamart D, Daëron M, Bar-Matthews M, et al. 2011. Speleothem record of the last 180 ka in Villars cave (SW France): investigation of a large δ¹⁸O shift between MIS6 and MIS5. Quat. Sci. Rev. 30(1–2):130–46
- Wang DT, Gruen DS, Lollar BS, Hinrichs KU, Stewart LC, et al. 2015. Nonequilibrium clumped isotope signals in microbial methane. *Science* 348(6233):428–31
- Wang Y, Passey B, Roy R, Deng T, Jiang S, et al. 2021. Clumped isotope thermometry of modern and fossil snail shells from the Himalayan-Tibetan Plateau: implications for paleoclimate and paleoelevation reconstructions. Geol. Soc. Am. Bull. 133(7–8):1370–80
- Wang Z, Nelson DD, Dettman DL, McManus JB, Quade J, et al. 2020. Rapid and precise analysis of carbon dioxide clumped isotopic composition by tunable infrared laser differential spectroscopy. Anal. Chem. 92(2):2034–42
- Wang Z, Schauble EA, Eiler JM. 2004. Equilibrium thermodynamics of multiply substituted isotopologues of molecular gases. Geochim. Cosmochim. Acta 68(23):4779–97
- Watkins JM, Devriendt LS. 2022. A combined model for kinetic clumped isotope effects in the CaCO₃-DIC-H₂O system. *Geochem. Geophys. Geosyst.* 23(8):e2021GC010200
- Watkins JM, Hunt JD. 2015. A process-based model for non-equilibrium clumped isotope effects in carbonates. Earth Planet. Sci. Lett. 432:152–65
- Winkelstern IZ, Lohmann KC. 2016. Shallow burial alteration of dolomite and limestone clumped isotope geochemistry. *Geology* 44(6):467–70
- Yanay N, Wang Z, Dettman DL, Quade J, Huntington KW, et al. 2022. Rapid and precise measurement of carbonate clumped isotopes using laser spectroscopy. Sci. Adv. 8(43):eabq0611
- Yeung LY, Young ED, Schauble EA. 2012. Measurements of ¹⁸O ¹⁸O and ¹⁷O ¹⁸O in the atmosphere and the role of isotope-exchange reactions. *7. Geophys. Res.* 117(D18):D18306
- Young ED, Kohl IE, Lollar BS, Etiope G, Rumble D III, et al. 2017. The relative abundances of resolved ¹²CH₂D₂ and ¹³CH₃D and mechanisms controlling isotopic bond ordering in abiotic and biotic methane gases. *Geochim. Cosmochim. Acta* 203:235–64

Zachos J, Pagani M, Sloan L, Thomas E, Billups K. 2001. Trends, rhythms, and aberrations in global climate 65 Ma to present. *Science* 292(5517):686–93

Zeebe RE, Wolf-Gladrow D. 2001. CO₂ in Seawater: Equilibrium, Kinetics, Isotopes. Amsterdam: Elsevier Zhang L, Wang C, Wignall PB, Kluge T, Wan X, et al. 2018. Deccan volcanism caused coupled pCO₂ and terrestrial temperature rises, and pre-impact extinctions in northern China. Geology 46(3):271–74



Annual Review of Earth and Planetary Sciences

Volume 51, 2023

Contents

Estella A. Atekwana
The Evolving Chronology of Moon Formation Lars E. Borg and Richard W. Carlson
Harnessing the Power of Communication and Behavior Science to Enhance Society's Response to Climate Change Edward W. Maibach, Sri Saahitya Uppalapati, Margaret Orr; and Jagadish Thaker53
River Deltas and Sea-Level Rise Jaap H. Nienhuis, Wonsuck Kim, Glenn A. Milne, Melinda Quock, Aimée B.A. Slangen, and Torbjörn E. Törnqvist
Machine Learning in Earthquake Seismology S. Mostafa Mousavi and Gregory C. Beroza
Bubble Formation in Magma James E. Gardner, Fabian B. Wadsworth, Tamara L. Carley, Edward W. Llewellin, Halim Kusumaatmaja, and Dork Sahagian
Continental Crustal Growth Processes Recorded in the Gangdese Batholith, Southern Tibet Di-Cheng Zhu, Qing Wang, Roberto F. Weinberg, Peter A. Cawood, Zhidan Zhao, Zeng-Qian Hou, and Xuan-Xue Mo
Iceberg Calving: Regimes and Transitions R.B. Alley, K.M. Cuffey, J.N. Bassis, K.E. Alley, S. Wang, B.R. Parizek, S. Anandakrishnan, K. Christianson, and R.M. DeConto
Fracture Energy and Breakdown Work During Earthquakes Massimo Cocco, Stefano Aretusini, Chiara Cornelio, Stefan B. Nielsen, Elena Spagnuolo, Elisa Tinti, and Giulio Di Toro
Evolution of Atmospheric O ₂ Through the Phanerozoic, Revisited Benjamin J.W. Mills, Alexander J. Krause, Ian Jarvis, and Bradley D. Cramer

Instructive Surprises in the Hydrological Functioning of Landscapes *James W. Kirchner, Paolo Benettin, and Ilja van Meerveld	7
Deconstructing the Lomagundi-Jatuli Carbon Isotope Excursion Malcolm S.W. Hodgskiss, Peter W. Crockford, and Alexandra V. Turchyn	1
Elastic Thermobarometry Matthew J. Kohn, Mattia L. Mazzucchelli, and Matteo Alvaro	1
Mimas: Frozen Fragment, Ring Relic, or Emerging Ocean World? Alyssa Rose Rhoden	7
The Mid-Pleistocene Climate Transition Timothy D. Herbert	9
Neogene History of the Amazonian Flora: A Perspective Based on Geological, Palynological, and Molecular Phylogenetic Data Carina Hoorn, Lúcia G. Lohmann, Lydian M. Boschman, and Fabien L. Condamine 41	9
Hydrological Consequences of Solar Geoengineering Katharine Ricke, Jessica S. Wan, Marissa Saenger, and Nicholas J. Lutsko	.7
What Models Tell Us About the Evolution of Carbon Sources and Sinks over the Phanerozoic Y. Goddéris, Y. Donnadieu, and B.J.W. Mills	1
The Rock-Hosted Biosphere Alexis S. Templeton and Tristan A. Caro	3
Petrogenesis and Geodynamic Significance of Xenolithic Eclogites Sonja Aulbach and Katie A. Smart	1
A Systems Approach to Understanding How Plants Transformed Earth's Environment in Deep Time William J. Matthaeus, Sophia I. Macarewich, Jon Richey, Isabel P. Montañez, Jennifer C. McElwain, Joseph D. White, Jonathan P. Wilson, and Christopher J. Poulsen	1
Ductile Deformation of the Lithospheric Mantle *Jessica M. Warren and Lars N. Hansen	1
Frontiers of Carbonate Clumped Isotope Thermometry Katharine W. Huntington and Sierra V. Petersen	1
Mars Seismology P. Lognonné, W.B. Banerdt, J. Clinton, R.F. Garcia, D. Giardini, B. Knapmeyer-Endrun, M. Panning, and W.T. Pike	.3
The Role of Giant Impacts in Planet Formation Travis S.J. Gabriel and Saverio Cambioni	1

Errata

An online log of corrections to Annual Review of Earth and Planetary Sciences articles may be found at http://www.annualreviews.org/errata/earth

Related Articles

From the *Annual Review of Astronomy and Astrophysics*, Volume 60 (2022)

Atmospheres of Rocky Exoplanets
Robin Wordsworth and Laura Kreidberg

From the *Annual Review of Chemical and Biomolecular Engineering*, Volume 13 (2022)

Direct Air Capture of CO₂ Using Solvents Radu Custelcean

Technological Options for Direct Air Capture: A Comparative Process Engineering Review Xiaowei Wu, Ramanan Krishnamoorti, and Praveen Bollini

From the Annual Review of Ecology, Evolution, and Systematics, Volume 53 (2022)

Evolutionary Ecology of Fire 7on E. Keeley and 7uli G. Pausas

Integrating Fossil Observations Into Phylogenetics Using the Fossilized Birth–Death Model

April M. Wright, David W. Bapet, Joëlla Barrida, Sottani

April M. Wright, David W. Bapst, Joëlle Barido-Sottani, and Rachel C.M. Warnock

The Macroevolutionary History of Bony Fishes: A Paleontological View Matt Friedman

From the Annual Review of Environment and Resources, Volume 47 (2022)

The Ocean Carbon Cycle

Tim DeVries

Permafrost and Climate Change: Carbon Cycle Feedbacks From the Warming Arctic

Edward A.G. Schuur, Benjamin W. Abbott, Roisin Commane, Jessica Ernakovich, Eugenie Euskirchen, Gustaf Hugelius, Guido Grosse, Miriam Jones, Charlie Koven, Victor Leshyk, David Lawrence, Michael M. Loranty, Marguerite Mauritz, David Olefeldt, Susan Natali, Heidi Rodenhizer, Verity Salmon, Christina Schädel, Jens Strauss, Claire Treat, and Merritt Turetsky

Remote Sensing the Ocean Biosphere Sam Purkis and Ved Chirayath

From the Annual Review of Fluid Mechanics, Volume 55 (2023)

Submesoscale Dynamics in the Upper Ocean

John R. Taylor and Andrew F. Thompson

Fluid Dynamics of Polar Vortices on Earth, Mars, and Titan

Darryn W. Waugh

Icebergs Melting

Claudia Cenedese and Fiamma Straneo

The Fluid Mechanics of Deep-Sea Mining

Thomas Peacock and Raphael Ouillon

Turbulent Rotating Rayleigh-Bénard Convection

Robert E. Ecke and Olga Shishkina

From the *Annual Review of Marine Science*, Volume 15 (2023)

From Stamps to Parabolas

S. George Philander

Sociotechnical Considerations About Ocean Carbon Dioxide Removal Sarah R. Cooley, Sonja Klinsky, David R. Morrow, and Terre Satterfield

Nuclear Reprocessing Tracers Illuminate Flow Features and Connectivity

Between the Arctic and Subpolar North Atlantic Oceans

Núria Casacuberta and John N. Smith

The Arctic Ocean's Beaufort Gyre

Mary-Louise Timmermans and John M. Toole

Global Quaternary Carbonate Burial: Proxy- and Model-Based Reconstructions and Persisting Uncertainties

Madison Wood, Christopher T. Hayes, and Adina Paytan

Quantifying the Ocean's Biological Pump and Its Carbon Cycle Impacts on Global Scales

David A. Siegel, Timothy DeVries, Ivona Cetinić, and Kelsey M. Bisson

Novel Insights into Marine Iron Biogeochemistry from Iron Isotopes *Jessica N. Fitzsimmons and Tim M. Conway*

Insights from Fossil-Bound Nitrogen Isotopes in Diatoms, Foraminifera, and Corals

Rebecca S. Robinson, Sandi M. Smart, Jonathan D. Cybulski, Kelton W. McMahon, Basia Marcks, and Catherine Nowakowski

Prokaryotic Life in the Deep Ocean's Water Column

Gerhard J. Herndl, Barbara Bayer, Federico Baltar, and Thomas Reinthaler

Lipid Biogeochemistry and Modern Lipidomic Techniques Bethanie R. Edwards

From the Annual Review of Materials Research, Volume 52 (2022)

Biomineralized Materials for Sustainable and Durable Construction Danielle N. Beatty, Sarah L. Williams, and Wil V. Srubar III

Brittle Solids: From Physics and Chemistry to Materials Applications Brian R. Lawn and David B. Marshall

Material Flows and Efficiency

Jonathan M. Cullen and Daniel R. Cooper

Architectural Glass

Sheldon M. Wiederhorn and David R. Clarke